ACDIS

Research Report

Intermediate Complexity Climate Economic Productivity Impact Model: Consequence of Failure to Limit Greenhouse Gas Emissions

Clifford E. Singer
Program in Arms Control & Domestic and International Security
University of Illinois at Urbana-Champaign

Research of the Program in Arms Control
& Domestic and International Security

University of Illinois at Urbana–Champaign

January 2024

The research for this publication is supported by the University of Illinois. It is produced by the Program in Arms Control & Domestic and International Security at the University of Illinois at Urbana-Champaign.

The University of Illinois is an equal opportunity/ affirmative action institution.

The ACDIS *Research Reports* series publishes technical reports and the findings from contracted grant research. For additional information and to download publications, visit the ACDIS home page at: http://acdis.illinois.edu/

Published 2024 by ACDIS//ACDIS SIN:1.2024

University of Illinois at Urbana–Champaign
101 Coble Hall, 801 S. Wright St.
Champaign, IL 61820

Series Editor: Rachitha Onkar

Intermediate Complexity Climate Economic Productivity Impact Model: Consequence of Failure to Limit Greenhouse Gas Emissions

CLIFFORD E. SINGER
csinger@illinois.edu
Program in Arms Control & Domestic and International Security
University of Illinois at Urbana Champaign

A relatively parsimonious set of climate change impact formulas has been designed for examining consequences of policy decisions. Included are impacts on economic productivity from changes in global and regional average temperature and atmospheric carbon dioxide concentration on agriculture, forestry, and HVAC (heating, ventilation, and air conditioning). The impact of sea level change is included because it is particularly significant for one of the sixteen geographical regions examined. Impacts of temperature change on diseases and storm damage are also included. Reduction of space heating costs and increases in agricultural productivity are overwhelmed in some regions by negative impacts as temperature increases. Carbon dioxide fertilization of agriculture and forestry is countered by coral reef damage and costs associated with direct impacts of elevated CO_2 concentrations on human productivity. One example is shown that has no implementation of new policies to further limit greenhouse gas emissions up to and beyond a time where economic impacts are becoming increasingly disadvantageous. Other examples allow for mitigation of carbon emissions or solar radiation management.

1. Motivation

Obtaining experimentally derived information relevant to expected future human response to climate change from simulation exercises [1] requires constructing an impact assessment analysis that is sufficiently realistic, but also transparent enough that participants can understand its implications during a tractable orientation period. These requirements are not consistent with general and partial equilibrium models with large numbers of market components, such as that of the Global Trade Analysis Project (GTAP) [2]. Of the various models reviewed by Stanton, Ackerman, and Kartha [3] and chosen for study by Gillingham et al. [4], other than RICE [5] and FUND [6] many were too complex for the present purposes. Application of formulas for impacts of climate change on economic productivity from Burke, Hsiang, and Miquel [7] would give results that differ substantially from those from the type of approaches used in FUND and herein. Here there is no attempt to resolve such discrepancies, just a caution that the type of analysis presented here could give very different results if the kind of approach used by Burke, Hsian, and Miquel were adopted. A framework based on the FUND 3.9 model [6, 8] was chosen over a recent version of the RICE model as a starting point because the FUND model separates impacts of changes in global average temperature and atmospheric carbon dioxide concentration. Such separation is needed in case the model described here is used for examination of solar radiation management (SRM) options [9, 10].

The FUND 3.9 model documentation describes impact estimates variously as changes in production, consumer and producer surplus, dollar value of a resource, expenditures, net present costs, value of a statistical life or year of morbidity, or economic damage. These are all converted here to percentage changes in gross domestic product. As in the RICE model, here it is assumed that economic impacts of climate change influence a gross domestic product (GDP) that has a component proportional to $bK^{1-\omega}L^{\omega}$ where b is productivity, K is time-varying capital stock, L is time-varying labor supply, and ω is referred to as the labor fraction of production. This is similar to the approach used in RICE models. However, here each region has a minor part of base total per capita GDP that is approximated as constant in time. The time-varying part of per capita GDP is referred to as incremental per capital GDP and denoted by the symbol y_r with the subscript r ranging over the sixteen geographic regions in the model. Also, the labor supply that contributes to the increment in per capita GDP over that constant base is proportional only to the increment in population over year the first year for which annual estimates of population were used, which is 1820. That population increment is denoted by the symbol P_r. The reasons for this approach and its method of implementation are described below and in a companion report [11]. Formulas and parameters for y_r and P_r are given below in Appendix C.

Here, productivity that contributes to the incremental per capita GDP is written as $b = (1+\epsilon D)a$, where a is a logistic function and $\epsilon = 0.01$. Values of D are thus percentages of fractional impacts on productivity. The symbol D is chosen as a reminder that negative values of D correspond to damage to economic productivity. The FUND 3.9 GDP impacts are based on assessments during a time when climate change was evolving slowly enough that the percentage impacts on GDP are assumed to be approximately equal to the changes in productivity divided by ω (c.f. Appendix C). For the purpose of drawing upon estimates of economic impacts of climate change, the differences between the FUND 3.9 base year of 1990 and a reference year 2019 used as a starting point for extrapolations here (c.f. Appendix B). Historical percentage changes in productivity are thus approximated here as equal to ω times percentage changes in GDP. The graphical results presented here are for percentage changes in productivity.

Herein, Section 2 gives a definition of the model components. Section 3 comments on rationale for choices of model components and their relationship to the FUND 3.9 model. Section 4 provides some results consistent with extrapolations of fits to sixteen geographical regions' per capita GDP and population and with extrapolations of atmospheric carbon dioxide concentration, $< CO_2 >$ [12] and global average temperature [13, 14]. That is supplemented with estimates of resulting sea level dependence on global average temperature following Grinsted, Moore, and Jevrejea [15] and dependence of coral reef loss on $< CO_2 >$ following Brander et al. [16]. Appendix A includes tables describing geographic regions. Appendix B lists values or sources for the original formulas and parameters used and describes approximations and simplifications used to obtain the description of the GDP impact model presented in Section 2. Appendix C lists parameters used for extrapolating per capita GDP and population fits to historical data and United Nations population extrapolation, for each region. Appendix D gives formulas for anthropogenic atmospheric emissions of carbon in the form of carbon dioxide.

2. Model Description

In this section, the geographic regions used are illustrated graphically. Three aspects of the model are described in different sections of this report. This section lists formulas and parameters used. Section 3 provides information why these formulas were chosen. Appendix B provides details that would be useful for someone who wanted to do calculations with such a model while constructing updated or alternative lists of the parameter values. Formulas are given in this section for evolution of percentages changes in productivity associated with changes in global average temperature, $< CO_2 >$, sea level, and fractional loss of coral reef areas due to surface ocean layer acidification. All of the impacts estimated are changes from reference year 1990.

2.1. **Geographic Regions.**

The sixteen geographic regions used here are illustrated in Figure 1. Table A1 lists, by International Standards Organization code [17], how countries and other UN reporting units are assigned to each region. Table A2 gives full names of some of the included reporting units. Table A3 lists what is included in the SIS (Small Island States) region. Some, but not all, reporting units not recognized by the United Nations as sovereign states are assigned to regions containing countries that they are associated with. The assignment of islands was generally based on geography for cases where adequate data on economic production was available and by political association otherwise.

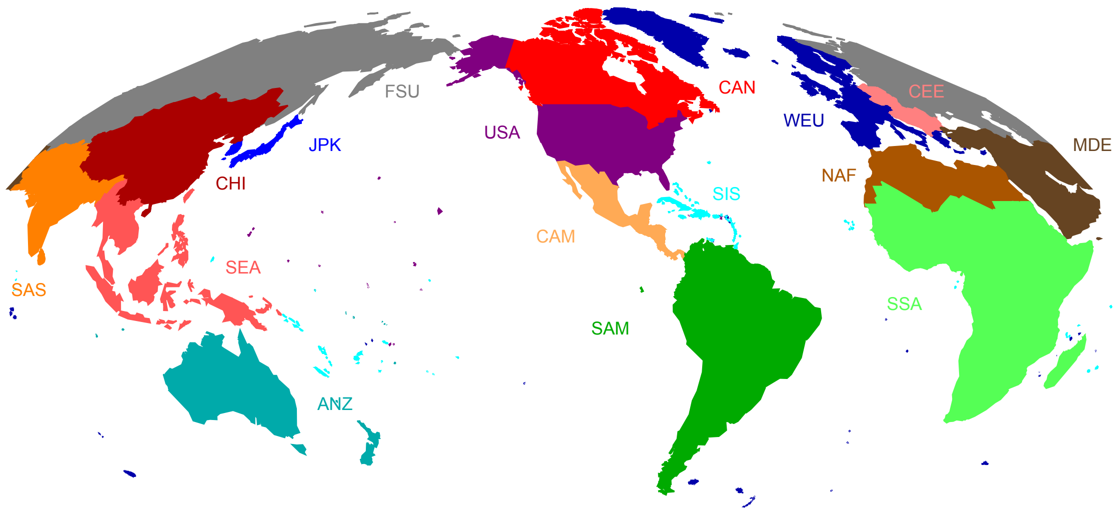

Figure 1. Geographic regions.

2.2. **Impact Formulas.** The formulas listed here contain both global and region-dependent parameters. Values of those parameters are collected in Tables 1–5. (The numbers of digits included throughout this report for numerical values are chosen to facilitate independent reproduction of the results with minimal concern about rounding truncations, not to represent underlying accuracies.) Each region has seventeen additive components of impact formulas. Each component of impacts on productivity for each region is equal in Julian year 2019 to the values (in units of percent) of ωc_r^{XY}, with values of c_r^{XY} listed in Table 4 and the formula for and rationale for use of the constant $\omega = 0.675$ described in and after Table C2. The second letter in the superscripts is T for impacts due to temperature changes and C for impacts due to changes in $< CO_2 >$.

For years $t_0 = 1990$ and beyond, the impacts on economic productivity are ωf_r^{XY}

$$f_r^{XY} = c_r^{XY}(y_r/y_{1r})^{\zeta_r} g_r^{XY}/g_{1r}^{XY} \tag{2.1}$$

for agriculture. For the other impacts, formulas for f_r^{XY} are

$$f_r^{XY} = c_r^{XY}(y_r/y_{1r})^{\epsilon_{XY}} 2^{-(t-t_1)/t_{1/2}^{XY}} g_r^{XY}/g_{1r}^{XY} \tag{2.2}$$

Here y_r are functions of time for each region that are proportional to increments of per capita production over a constant base levels, and y_{r1} are the values of y_r for Julian year 2019. The formulas and parameter values defining y_r are in Appendix C. The formulas and parameters for the increments P_r of population over a base value for each region that are referred to in row WT of Table 1 are also in Appendix C.

Functional dependences on global average temperature and $< CO_2 >$ are listed in Table 1. There are equations below for Σ_r and R, used for sea level and coral reef damage respectively. All of the expressions for g_r^{XY} are independent of the region r, except for g_r^{WT} (for water) and g_r^{OT} (for sea level).

Table 1. Impact Formula Constants and Functions, with $T = \tau - \tau_0$

XY	ϵ_{XY}	$t_{1/2}^{XY}$(yr)	g_r^{XY}	Type
RT			$(\tau')^2 - (\tau'_0)^2$	agriculture
LT			T	agriculture
QT			T^2	agriculture.
AC			$\ln(< CO_2 > / < CO_2 >_0)$	agriculture
FT	- 0.31	0	T	forestry
FC	-0.31	0	$\ln(< CO_2 > / < CO_2 >_0)$	forestry
WT	-0.15	138.6	$(P_r/P_{1r})^{\epsilon_{WT}}T$	water
HT	-0.20	0	$\mathrm{ArcTan}(T)$	heating
CT	-0.20	0	$\tau^2 - \tau_0^2$	cooling
VC	-1	0	$< CO_2 > - < CO_2 >_0$	ventilation
OT	0	0	$\Sigma_r - \Sigma_{0r}$	sea level
OC	0	0	$R - R_0$	coral reefs
DT	-1.58	30	T	mortality
MT	. -0.42	30	T	morbidity
VT	-2.65	16	T	vectors
ST	-0.514	0	T	property damage
KT	-0.501	0	T	storm deaths

The value used in Table 1 for $< CO_2 >$ in 1990 is $< CO_2 >_0 = 353.3$ ppm (parts per million by volume) [12]. The function of time τ is the difference in annually and globally average temperature from the temperature that would be in thermal equilibrium with radiative forcing averaged over 11 years centered on Julian year 1750. The function $T = \tau - \tau_0$ with $\tau_0 = 0.7151°$C. A prime indicates annual rate of change, and the value of τ' in 1990 is $\tau'_0 = 0.0166°C/\mathrm{yr}$. These values were calculated by solving a first order differential global heat balance equation containing parameters fitted to historical data [18].

Here, 0 and 1 in a subscript refer to Julian years 1990 and 2019 respectively. For example, the notation g_{1r}^{XY} refers to the values of the functions g_r^{XY} in Table 1 evaluated for year t_1=2019. Values for income elasticities ϵ_{XY} and the half-lives $t_{1/2}^{XY}$ of the water supply and medical technology improvement timescales are listed in Table 1. Values of the region-dependent percentage impacts c_r^{XY} on GDP in 2019 are listed below in Table 4. Values of other constants referred to in Section 2 are listed in Tables 2, 3, and 5.

The constants ϵ_{XY} in the formulas for f_r^{XY} are referred to here as elasticities with respect to per capita GDP. For agriculture, income elasticities are the different values of ζ_r listed in Table 2. The constants ζ_r are coefficients from log-linear fits to data from the Food and Agriculture Organization (FAO) [19] and GDP for each region, as described in Appendix B and listed in Table B1. The other constants ϵ_{XY} listed in Table 1 are the same for each region.

Table 2. Agriculture Fraction vs. per Capita GDP Exponents ζ_r

USA	CAN	WEU	JPK	ANZ	CEE	FSU	MDE
-0.769	-0.669	-1.002	-0.942	-0.894	-1.045	-0.573	-0.919
CAM	SAM	SAS	SEA	CHI	NAF	SSA	SIS
-0.680	-0.218	-0.715	-0.558	-0.530	-0.568	-0.711	-1.446

In Table 1, a formula used for sea level impacts is

$$\Sigma_r = (1+\sigma_r) H_m^{\sigma_r} (\tau - \tau_S) \tag{2.3}$$

where $H_m = H/(1\,m)$ and $H = H_0 + S$. The expression

$$S = a_S \int_{t_0}^{t} (\tau - \tau_S) dt \tag{2.4}$$

gives the change of global sea level in meters since 1990, $\tau_S = 0.1626°\text{C}$ is the value of τ at which sea level would be in equilibrium, and $a_S = 0.0063$ (m/°C)/yr. For the formulas in Table 1, $H_0 = 0.26$ m is the increase in sea level in meters from 1750 to 1990 [13, 15]. (The denominator of 1 m is included in the definition of H_m to make the formulas dimensionally correct.) Values of the exponents σ_r are listed in Table 3.

Table 3. Sea Level GDP Exponents σ_r

USA	CAN	WEU	JPK	ANZ	CEE	FSU	MDE
-0.417	-0.749	-0.727	-0.588	-0.452	-0.807	-0.445	-0.372
CAM	SAM	SAS	SEA	CHI	NAF	SSA	SIS
-0.322	-0.244	-0.070	-0.188	-0.292	-0.663	-0.201	-0.333

The global coral reef survival fraction R of year 1750 coral reef area, as used in the formula for g_r^{OC} in Table 1, is

$$R = \gamma_{OC} A_{OC} / (1 + \gamma_{OC} A_{OC}) \tag{2.5}$$

where γ_{OC}=0.56 (pH units)$^{-1}$. The absolute value of the change pH units of upper ocean acidity from 1750 is

$$A_{OC} = \alpha_{OC} (< \text{CO}_2 > - < \text{CO}_2 >_{OC})^{\beta_{OC}} \tag{2.6}$$

with $\alpha_{OC} = 0.00569$, $\beta_{OC} = 0.67$ and $< \text{CO}_2 >_{OC}$=280 ppm [16].

The values of τ_0, τ_0', $< \text{CO}_2 >_0$, τ_S, H_0, a_S, the population and per capita GDP parameters listed in Appendix C, and thus c_r^{XY}, depend on the models of historical data drawn upon for this study [12, 18], as described in more detail in a companion report [11]. Those parameters are fixed for the present study, but the fixed values of c_r^{XY} would be different if the method for evaluating them that is described in Appendix B were changed by an investigator who used different model parameters than drawn upon here.

Some of the formulas in the FUND 3.9 model documentation depend on regional average temperature, and some depend on global average temperature, as described in Appendix B. Here, constant ratios of regional to global average temperature have been absorbed in the values of c_r^{XY} listed in Table 1. That helps to simplify the form of the equations for f_r^{XY}.

Table 4. Productivity impact coefficients c_r^{XY}

	USA	CAN	WEU	JPK	ANZ	CEE	FSU	MDE	Type
AR	-.0097	-.0028	-.0013	-.0004	-.0011	-.0016	-.0020	-.0010	ag $(\tau')^2$
AL	.0342	.2010	.0214	.0171	.0985	.0839	.1205	.0549	ag T
AQ	-.0111	-.3026	-.0090	-.0055	-.0224	-.0216	-.0348	-.0151	ag T^2
AC	.0666	.0405	.0903	.0554	.1809	.0097	.1016	.0724	ag CO_2
FT	.0013	.0003	.0006	.0011	-.0030	.0014	-.0007	0	forestry T
FC	.0004	8E-5	.0002	.0003	-.0009	.0004	-.0002	0	forestry CO_2
WT	-.0311	-.0273	-.1331	.0001	.0001	-.3394	-1.1416	-.0602	water
HT	.2635	.2347	.1497	.1282	.0906	.2750	.2954	.2028	heating
CT	-.0868	-.0770	-.1540	-.0120	-.0084	-.0744	-1.0934	-.0962	cooling
VC	-.0135	-.0166	-.0180	-.0206	-.0184	-.0346	-.0483	-.0408	ventilation
OT	-.0003	0	0	-.0141	-.0138	0	0	-.0040	sea level
OC	-4E-5	0	0	-.0003	-.0191	0	0	-.0009	reef loss
DT	-.0144	-.0193	-.0054	-.0003	-2E-5	-.0054	-.0791	-.0109	mortality
MT	-.0042	-.0053	-.0015	-.0004	-.0002	-.0020	-.0207	-.0004	morbidity
VT	-2E-6	-3E-6	-3E-5	-.0003	-1E-6	-4E-5	-5E-5	-.0028	vectors
ST	-.0084	-.0005	-.0006	-.0019	-.0041	-.0001	-.0003	-4E-5	property
KT	-.0073	-4E-5	-7E-5	-.0011	-.0003	-3E-5	-.0001	-3E-5	storm deaths

	CAM	SAM	SAS	SEA	CHI	NAF	SSA	SIS	Type
AR	-.0012	-.0006	-.0010	-.0003	-.0016	-.0012	-.0014	-.0010	ag $(\tau')^2$
AL	.0886	.0085	.0642	.0191	.1462	.0707	.1190	.0397	ag T
AQ	-.0215	-.0057	-.0151	-.0057	-.0403	.-0202	-.0256	-.0069	ag T^2
AC	.1751	.1343	.1114	.1105	.3740	.0924	.1934	.1980	ag CO_2
FT	.0005	.0006	.0008	.0013	.0012	0	.0003	0	forestry T
FC	.0001	.0002	.0002	.0004	.0004	0	.0001	0	forestry CO_2
WT	-.0619	-.0669	-.0519	-.1301	.2016	-.4036	-.1651	-.0622	water
HT	.0670	.0805	.0377	.0076	1.6358	.0090	.0039	3E-5	heating
CT	-.1013	-.1084	-.1030	-.2580	-.7938	-.7564	-.3467	-.0990	cooling
VC	-.0521	-.0557	-.1615	-.0641	-.0516	-.0806	-.5056	-.0696	ventilation
OT	-.0044	-.0004	-.0026	-.0491	-.0003	-.0015	-.0014	-.4754	sea level
OC	-.0010	-.0003	-0004	-.0072	-5E-5	-.0010	-.0047	-.0648	reef loss
DT	-.0550	-.0500	-.0022	-.0079	-.0005	-.1157	-1.3205	-.0607	mortality
MT	-0013	-.0012	-.0007	-.0007	-,0004	-.0022	-.0118	-.0017	morbidity
VT	-.0005	-.0005	-3E-5	-.0003	-1E-5	-.0425	-.3100	-.0117	vectors
ST	-.0108	-.0001	-.0043	-.0016	-.0040	-7E-7	-.0021	-.0361	property
KT	-.0001	-.0001	-.0002	- 3E-5	-2E-5	-2E-5	-.0001	-.0028	storm deaths

Table 5. Miscellaneous Impact Formula Constants

Symbol	Value	Units	Meaning
τ_0	0.7151	°C	τ in 1990
τ'_0	0.0166	°C/yr	τ' in 1990
$< CO_2 >_0$	353.3	ppm	$< CO_2 >$ in 1990
H_0	0.26	m	Sea level increase from 1750 to 1990
τ_S	0.1626	°C	τ for constant sea level
a_S	0.0063	(m/°C)/yr	Seal level change coefficient
α_{OC}	0.00569	(pH units)/ppm$^{\beta_{OC}}$	Acidification coefficient
β_{OC}	0.67	1	Acidification exponent
γ_{OC}	0.56	(pH units)$^{-1}$	Reef damage coefficient
$< CO_2 >_{OC}$	280	ppm	Acidification baseline $< CO_2 >$
R_0	0.909	1	Global coral reef survival fraction in 1990

3. Rationale for Impact Model Components

Using differences from year 1990 for impacts on GDP is convenient for two reasons, one practical and one conceptual. The practical reason is that using differences from 1990, similarly to the FUND 3.9 model, simplifies explaining the formulas used. The conceptual reason is that a clear trend of increasing τ from the 1990s on emerged from variations around a 1980s mean temperature that followed three decades of substantially slower increase in τ [18]. The conceptual context used here has adaptation to anthropogenic climate change effects on GDP relatively small compared to other influences on economic development before about 1990, but becoming appreciable enough thereafter to be useful to analyze.

Another choice made here is avoiding use of data and analysis thereof for years after 2019. This also involves practical advantages and an underlying conceptual framework. Compared to regularly updating using latest data from the various years it is available for calibrating models for τ, $< CO_2 >$, S, R, y_{XY}, and P_{XY}, the approach adopted here is both simpler and avoids dealing with variable lags between the latest year for which some data is available and the number of years for which availability of other data lags behind that year. The conceptual framework used here is based on the idea that global and regional perturbations associated with the international spread of COVID-19 from 2020 and war in Europe from 2022 will end up being as transient as previous perturbations between 1990 and 2020. Whether that proves to be the case in the longer term remains to be revealed, but figure 3 in a companion report [11] suggests that this idea has been reasonable at least for the short term. What is clear is that detailed modeling of such effects and their implications for temporal extrapolations is incompatible with the above-mentioned goal of providing a model that is close in simplicity and transparency to the one presented here.

The model described here was assembled to provide a framework to pose some interesting questions about economic impacts, not to provide answers based either on a fixed set of model parameters or on sampling of probability distributions for those parameters. This in in contrast to the inclusion of probability distributions for model parameters in the Framework for Uncertainty, Negotiation, and Distribution [6]. Some insight into uncertainties about many of the parameters in the present model can nevertheless be gathered from the FUND 3.9 documentation.

The following subsections describe some of the overall rationale behind the formulation used here for different groups of economic impacts of climate change. Then comes a summary of economic impacts of expenditures for limiting anthropogenic CO_2 emissions, inter-regional for paying for those expenditures, and direct costs of implementing solar radiation management. At the end of this Section comes a discussion of the reasons for differences in income elasticity and some comments on the role of adaptation. Appendix B provides information meant to be detailed enough to allow revisions of the model based on different choices for parameters in the FUND 3.9 documentation and other literature referenced.

3.1. **Agriculture, Forestry, and Water.**

3.1.1. *Agriculture.* Increases in $T = \tau - \tau_0$ from 0 in 1990 initially make a positive contribution to agricultural production. However, the f_r^{LT} terms that have g_r^{LT} linear in T in Table 1 are offset by terms quadratic in T if the temperature gets high enough. Depending on whether the absolute value of the rate of change τ' of temperature larger or smaller than that in 1990, then there is respectively an additional negative or positive, but much less important, contribution f_r^{RT} that reflects costs of adapting agricultural practices to changes in temperature.

Increasing $< CO_2 >$ in the model has a positive effect on the contribution to GDP from land-based agriculture for each region taken as a whole. For regions with valuable coral reefs, $< CO_2 >$ fertilization of land-based agriculture faces a countervailing effect from damage to coral reefs.

3.1.2. *Forestry.* Increasing $< CO_2 >$ has a positive economic effect on forestry in each region, except for the former Soviet Union (FSU) and Australia and New Zealand (ANZ). However, both forestry effects on fractional changes of GDP are much smaller in magnitude than the corresponding effects on agriculture.

3.1.3. *Water.* Climate change is expected to affect regional patterns of precipitation and evapotranspiration and thus availability and cost of water supplies. As noted in a report from the Intergovernmental Panel on Climate Change (IPCC) [20], there has been considerable uncertainty about details of the anticipated regional distribution of changes between precipitation and evapotranspiration through the twenty-first century. For the FUND 3.9 model, all but one of the water resource impacts are either very close to zero or negative. The FUND 3.9 exception is a large positive impact for China. There is also a substantial negative impact for the FSU region. These impacts are discussed further in the Example Results Section below.

3.2. **Heating, Cooling, and Ventilation.**

3.2.1. *Heating and Cooling.* Increasing temperature reduces costs of space heating. However, if it gets warm enough then no space heating is needed. As in FUND 3.9, the resulting saturation of cost savings for space heating with respect to the year 1990 is modeled here with an ArcTan(T) function.

The cost of space cooling per °C of temperature reduction increases with the difference between the outside temperature and the inside temperature. In FUND 3.9, this effect is modeled here with a $(\tau - \tau_0)^{3/2}$ function. To allow for the possibility of cooling below temperature τ_0 with consequent $T = \tau - \tau_0 < 0$, here that function is replaced with one proportional to $\tau^2 - \tau_0^2$. That replacement matches the FUND 3.9 result when τ is equal to the temperatures in 1990, 2019, and if τ reaches 4.19°C.

Not all of the economic impact of human exposure to lower or higher temperatures is dealt with by space heating or cooling. Here is assumed that the economic impacts of exposure to such temperatures is the same as the cost of controlling exposure to those temperatures, because the alternative of exercising that control is implicitly assumed to be available. This is a substantial idealization, but it simplifies the model without delving into details of the economic impacts of human exposure to temperature changes by other means than changing space heating and cooling.

Unlike with water supply (and unlike in the FUND 3.9 model), here there is no technological efficiency improvement as a function of time for space heating and cooling. Before population growth and industrial uses put increasing stress on the common practice of treating water as an allocated free good, there is assumed here to have been a shortage of incentives for technological progress in the water supply sector to keep up with technological progress in the broader economy. In the energy sector, by contrast, regulatory barriers and sporadic cooperation amongst exporters produced price pressure that stimulated technological improvements. There are also intrinsic physical limits to energy efficiency, so some of the time-dependent autonomous energy efficiency improvements (AEEI) in tables of externally generated AEEI scenarios reported for FUND 3.9 may not be realized. Avoiding AEEI scenarios here both simplifies the model and pays attention to differences between water and energy supplies. While it may be maintained that it is also physically impossible for water supply efficiency to approach infinity asymptotically with time, the approximately 139 year half life in the water supply efficiency factor used here (and in FUND 3.9) is longer than the remaining time in twenty-first century where important decisions concerning future evolution of $< CO_2 >$ and τ may be particularly pressing.

3.2.2. *Ventilation.* Since the documentation of the FUND 3.9 model became available, there has been more recent research on the impact of CO_2 exposure on human cognitive function [21, 22]. Increasing levels of outdoor $< CO_2 >$ increase the cost of ventilation needed to limit the impact of CO_2 on people in enclosed spaces. If outdoor $< CO_2 >$ becomes large enough, it becomes impractical to control inside exposures by increasing ventilation without also scrubbing CO_2 from inside air. To simplify this complicated picture, the model used here is based on the cost [23] of removing from a standard outside air intake rate the part $(< CO_2 > - < CO_2 >_0)$ of the outside ambient CO_2. As detailed in Appendix B, the air intake rate is based on establish ventilation standards [24] in $(l/s)/m^2$ times a reference m^2/person of indoor space [25]. As with space heating and cooling above, for situations where human exposure to CO_2 is not in fact controlled it is implicitly assumed that the productivity cost of not doing this is equal to the cost outlay for doing so. In practice, CO_2 scrubbing is more likely to be used first in work environments large enough to need active ventilation control systems in any case. That kind of situation is more likely to have costs that scale with annual scrubbing amounts, in contrast with costs dominated by paying for ventilation systems that would otherwise not normally be installed. For situations where the outside $< CO_2 >$ level is low enough to allow the possibility of increasing ventilation rates instead of scrubbing CO_2, or to accept human exposure to increasing CO_2 rather than limiting that exposure, the same linear model linear model with cost in proportion to $(< CO_2 > - < CO_2 >_0)$ is nevertheless used for simplicity. Note that the ventilation impact is linear in $(< CO_2 > - < CO_2 >_0)$, while the CO_2 fertilization effect is proportional to the logarithm of $< CO_2 > / < CO_2 >_0$. Thus, in the long run if $< CO_2 >$ increases enough, the combination of these effects in this model can become negative.

3.3. **Sea Level and Coral Reef Loss.**

3.3.1. *Sea Level.* The FUND 3.9 model has a complex set of interactions between coastal protection and loss of dry land and wetlands. The simplification used here accounts only for the rate of loss of dry land. Additional loss of wetlands and partially compensating coastal protection efforts are omitted for simplicity. The overall extrapolated effect of sea level rise is much smaller than the sum over all other negative effects of increasing global average temperature, except for the Small Island States (SIS) as discussed in the Example Results Section below.

It is the rate of land loss, e.g. due to loss of improvements that have not fully depreciated, that is assumed here to affect GDP. Each region is assumed to have a large enough overall supply of land on which to replace those assets that there is not a permanent impact on GDP from flooding of coastal land, (This approach implicitly assumes that political barriers will ultimately prove to have limited effectiveness in limiting migration of people within each region; c.f. comments on migration below.) The exponents σ_r in Table 3 reflect geographic information on how much more rapidly than linearly land elevation increases with distance from the coast.

3.3.2. *Coral Reef Loss.* The FUND 3.9 model includes an estimate of the global cost of biodiversity reduction as a function of global average temperature. It assigns the total cost in proportion to the GDP of each region, divided by a function of per capita GDP. While anthropogenically driven species extinction has recently gained global attention, it is difficult to untangle how much can be ascribed to changes in global average temperature versus other human activities. To tie ecosystem effects to more directly quantifiable costs associated with anthropogenic climate change, the present approach instead uses estimates of the cost of coral reef loss as a function of upper ocean acidification. Fractional loss of preindustrial reef area listed above is $R = 0.56A_{OC}/(1 + 0.56A_{OC})$, with acidity changes $A_{OC} = 0.00569(< \mathrm{CO_2} > - < \mathrm{CO_2} >_{280})^{0.67}$. (The baseline preindustrial $< \mathrm{CO_2} >$ from the reference for this formula [16] is $< \mathrm{CO_2} >_{280}$=280 ppm.) Additional coral reef damage due to ocean temperature increases is not accounted for. This implicitly, and quite possibly optimistically, assumes that some combination of local controls of ocean temperature and reseeding reefs with coral varieties or species adapted to higher temperatures is feasible. As with sea level rise, the purpose of this approach is to suggest where impacts on wild species might have particular identifiable economic impact, rather than to provide a more complete quantitative model of the economic impact of overall ecosystem changes.

3.4. **Diseases.** Impacts of temperature modeled include mortality and morbidity from diarrhea, and mortality from three vector-bone diseases. Those vector-borne diseases are malaria, dengue fever, and schistosomiasis. Increasing regional average temperature tends to make economic impacts more negative for all of these except schistosomiasis. However, the impact of malaria dominates over that of schistosomiasis in all sixteen regions. Increases of regional per capita GDP are taken to reduce the percentage change in GDP due to all of these diseases. However, there are also more globally distributed efforts to control these diseases, notably but not exclusively in the case of malaria. Included in Table 1 are thus estimates [26, 27] of the inverses of half-lives for decline of the economic impact of included diseases to continue in addition to effects of regional increases in per capita GDP.

Not included here is an effect of changes in regional average temperatures on deaths from cardiovascular disease. While deaths associated with weather that produces large temperature excursions are sometimes well publicized, they can be avoided to some extent by improvements in space heating and cooling and adaptations of human behavior [28]. It is assumed here that the cost of controlling cardiovascular deaths associated with regional temperature changes is subsumed in the space heating and cooling costs described above. For heating, ventilation, and air conditioning (HVAC) in general, it is implicitly assumed that human health impacts from sub-optimal spending on HVAC are comparable to the costs that would be associated with otherwise extrapolated HVAC costs.

3.5. **Storm Damage.** Both property damage and mortality from tropical and extratropical storms are included. For extratropical storms, the FUND 3.9 model has damage in proportion to increases in $< \mathrm{CO_2} >$ over a preindustrial level. For applications where increases in radiative forcing from $\mathrm{CO_2}$ are balanced by decreases in other contributions to radiative forcing (e.g. using anthropogenic stratospheric sulfur injection), that approach would be problematic. Here, using equations in Appendix B, the FUND 3.9 climate change driving term for extratropical storms after 2019 is proportional to $T = \tau - \tau_0$ and scaled to match the FUND 3.9 result for Julian year 2019.

The income elasticities for property damage and mortality from storms in FUND 3.9 are only slightly different. Nevertheless, different entries for property damage and mortality from storms are included to give an idea of which of property damage and mortality is estimated to have more impact on GDP.

3.6. **Carbon Emissions Limitations, Transfers, and SRM.** The percentage impact on productivity of multiplying extrapolated anthropogenic atmospheric carbon emissions from region r

by a a time-dependent function $f_r < 1$ is

$$D_{Er} = -\omega\alpha_E(1-f_r)^{\beta_E}(1+f_{\mathrm{get},r}) \tag{3.1}$$

where $f_{\mathrm{get},r}$ =Min$[f_{Tr}, 0] < 0$ if and only if region r receives transfer payments. Here F_{Tr} are input constants, and the constants $f_{\mathrm{give},r}$ =Max$[f_{Tr}, 0]$ used below are positive for regions that provide transfer payments. Estimates of $\alpha_E = 3.76$ and $\beta_E = 1.86$ are from a least squares fit to the middle of U.S. Congressional Budget Office estimates of GDP reduction [29] as a function of the emissions reduction fraction estimated for application of emissions caps in the 2019 American Clean Energy Act draft legislation H.R. 2454 [30], from Julian year 2015 through 2050. The percentage impact on productivity for the paying regions is given by

$$D_{Tr} = -\omega\Sigma_{\mathrm{pay}}f_{\mathrm{give},r}/G_{DP,r} \tag{3.2}$$

where

$$\Sigma_{\mathrm{pay}} = \alpha_E\sum_r(1-f_{g,r})^{\beta_E}f_{\mathrm{get},r}G_{DP,r} \tag{3.3}$$

Here $G_{DP,r} = P_r y_r$ for each of the sixteen regions, using the formulas and parameter values for P_r and y_r given in Appendix C.

The annual rate in MtonneS/yr of stratospheric sulfur injection required to produce a radiative shielding of ΔF is approximated, and the impact on productivity of the region paying for the direct cost of the sulfur injection is estimated, as follows: The results presented here depend on the time rate of change τ'_{noSRM} of τ as plotted in Figure 2a, the radiative forcing F_Σ corresponding to the evolution of $<CO_2>$ and other historically calibrated contributions to radiative forcing [31]. with SRM the temperature and total radiative forcing, stratospheric sulfur injection rate, and productivity impact on the a region r paying for the direct cost thereof out of its gross domestic product $G_{DP,r}$ evolve as

$$\tau_{\mathrm{SRM}} = \int_{t_1}^{t} g_s\tau'_{\mathrm{noSRM}}\,dt \tag{3.4}$$

$$g_s = 1-u(g_{s6},g_{s7})+u(g_{s6},g_{s7})(1+g_{s1}u(g_{s2},g_{s3})-(1+g_{s1})u(g_{s4},g_{s5})) \tag{3.5}$$

$$F_\Sigma - \Delta F = (c_{th}\tau'_{\mathrm{SRM}} + \tau_{\mathrm{SRM}}/\lambda) \tag{3.6}$$

$$S_{\mathrm{SRM}} = -S_{\mathrm{ref}}\ln[1-\Delta F/F_{\mathrm{type}}] \tag{3.7}$$

$$D_{Sr} = -\omega(c_{SRM}/\epsilon)S_{\mathrm{S}}/G_{DP,r} \tag{3.8}$$

where $t_1 = 2019$. Below, with the discussion of Table 6, are listed values of the seven constants g_{sk} and of S_{ref}, F_{type}, c_{SRM} used to produce the example results in that table. The global heat balance parameters used here [18] are $c_{th} = 28.49$ (W/m^2)/°C and $\lambda = 0.5175$°C/(W/m^2). The inclusion of $\epsilon = 0.01$ in the denominator here converts the values of D_{Sr} to percents. To avoid a singularity as $1-\Delta F/F_{\mathrm{type}}$ approaches zero a modification of these formulas is used, but for the example with results listed in Table 6 that correction is tiny enough to be a computational underflow and thus is not included here.

3.7. **Income Elasticities.** Except for agriculture, ventilation, sea level, and coral reefs, the income elasticities ϵ_{XY} listed in Table 1 come from the FUND 3.9 documentation, appropriately interpreted as described in Appendix B. Region-dependent elasticities for the agricultural fraction of GDP are included because many of them differ substantially from a globally uniform elasticity as used in the FUND 3.9 model. (Here, income elasticity refers to per capita income.) Ventilation costs are per capita and assumed to be constant after adjusting for inflation, so their fraction of GDP evolves inversely with per capita GDP. Percentage GDP impacts from annual changes in seal level are assumed to be proportional to annual land losses divided by a total land area that is approximated as constant. This in effect assumes that the cost of annual land loss per square kilometer increases with GDP, i.e. that use of coastal land is treated as a luxury good. This accounts for the zero entry in Table 1 for ϵ_{OT}. For coral reef loss, Brander et. al. [16] refer to coral reefs as a luxury good. Here we interpret this simply as an income elasticity of $\epsilon_{OC} = 0$. Estimates from comparisons of recent studies of different geographic regions [16] would instead convert here to income and population density elasticities of approximately 0.1 and -0.5 respectively. Those studies differ from the time series approach used here for agriculture. For population density in particular, the number of people per square kilometer of land is influenced by the very different total land areas of the geographical regions included. So here, for simplicity, the elasticities for sea level damage with respect to income and population are both set to zero.

3.8. **Uncertainty and Adaptation.** The FUND 3.9 documentation contains extensive notations on uncertainties in model parameters, albeit without comment on whether how parameter samples vary from nominal estimates would be expected to correlate [6, 8]. For some parameters, e.g. the WT, HT, and CT (water, heating, and cooling) constants above in Table 4, standard deviations listed in the FUND 3.9 documentation are equal to the absolute values of the parameters. For some of those parameters (e.g. HT and CT), the signs of the parameters can be expected to be known a priori. A comparatively simple way of addressing uncertainty about productivity impacts in the present model is to multiply parameters in Table 4 by a value of x sampled from a log-normal distribution $e^{-(\ln x/\sigma)^2/2}/(x\sigma\sqrt{2}\pi)$. Then, for example, choosing values for σ of 0.5, 1, or 1.5 suggest higher, intermediate, or lower confidence in the accuracy of the parameter values listed in Table 4. Options are then to use the same value of x to multiply all of the entries in Table 4, a different sample for each region, or a different sample for each impact type. It would also be possible to do this for different samples of a quadrivalent normal approximation to parameters that determine the evolution of global average temperature for a given future for anthropogenic atmospheric carbon emissions [13].

Even with a similar expected values of outcomes for a given emissions trajectory, uncertainty can influence what trajectory is actually chosen. Using an earlier version of the model described here, Chen used small group experiments to illustrate how group decision making can be influenced by participants' predilections toward confirmation of their own ideas or group conformity. Stronger conformity bias correlated with lengthier decision times [32]. While the influence of outcome uncertainty was not investigated in her experiments, higher levels of uncertainty might be expected to weaken the influence of confirmation bias. Another possibility, which remains to be investigated in the present framework, is that higher levels of uncertainty may prod those with confirmation bias to stress lower probability but high consequence outcomes. It is a large leap from small group simulations to outcomes of actual international interactions, and in any case conducting such simulations lies outside of the scope of the present report. However, the underlying principle is that uncertainty concerning outcomes can reasonably be expected to have an influence in international cooperation, or lack thereof, concerning climate change policy.

A common theme here is that adaptation strategies can limit economic costs of climate change below what those costs would be without adaption. Agricultural crops and equipment can be modified, leaving modest impacts associate with the rate of change of τ as long as those changes are not too rapid. Changes in space cooling can help control direct health effects of human exposure to higher temperature. Changes in ventilation systems can help limit effects on human cognitive function from exposure to higher CO_2 concentrations. Changes in zoning regulations and internalizing costs of insuring property damage from sea level increase and storms can limit the larger costs than would be incurred without those measures. Coral reefs can be protected, at least in part, from changes in global average temperature. Adaptation strategies potentially allow global technological progress on controlling diseases to be used by populations of affected countries. Migration between regions can *in principle* overcome economically inefficient attempts to fragment labor markets and help to make up for the costs of resettling migrants, but may at most only just do if not handled in a way that addresses concerns of residents of areas receiving immigrants.

The use of the above-mentioned assumptions about adaptations leads to lower impacts on gross domestic product (GDP) than would follow from the opposite approach of assuming no such adaptations. For example, estimating damage in low lying parts of metropolitan ares by wiping away the un-depreciated value of all current low-lying developed property results in much larger economic impacts than replacing that value elsewhere over time. Assumptions about optimal implementation of adaptation strategies can be expected to be overly optimistic. Nevertheless, results in the following Section for data-calibrated extrapolations of anthropogenic atmospheric carbon emissions, $< CO_2 >$, and τ, lead eventually to increasingly negative impacts on GDP in the absence of implementation of new policies for limiting those carbon emissions or otherwise limiting increases in global average temperature.

4. Example Results

Here, results are shown based on the above formulas, extrapolations of τ and $<CO_2>$ shown in Figure 2, and the formulas for per capita GDP and population by region given in Appendix C. The carbon emissions formula used for extrapolation of historical trends is described in Appendix D. An important caveat is that everything discussed here is in the context of one particular extrapolation calculation, not many other possible analysis methods.

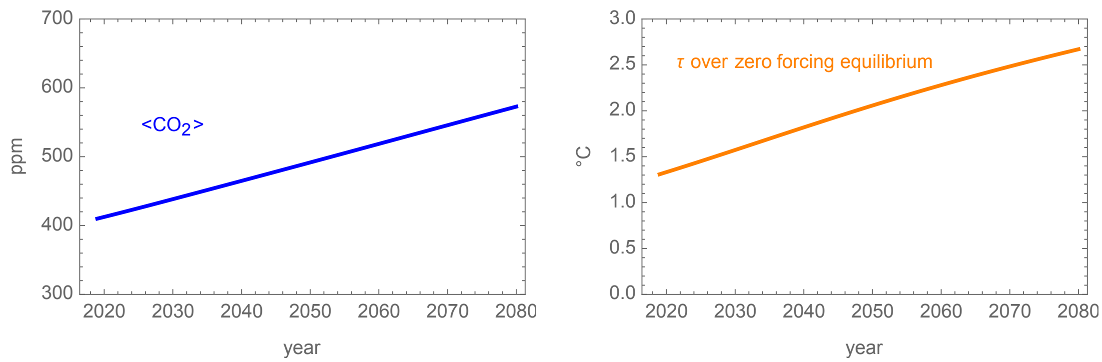

Figure 2. (a, left) Increase of global average temperature over a value $\tau = 0$ that would be in equilibrium with the radiative forcing averaged over 11 years centered on Julian year 1750 and (b, right) evolution of atmospheric carbon dioxide concentration $< CO_2 >$.

4.1. **Economic Impact Extrapolations.** The following figures plot climate change impacts on productivity as functions of time. For the evaluation of extrapolated productivity impacts ωf_r^{XY}, extrapolations are needed for the ratio of each region's incremental per capita GDP, y_r, and population, P_r increment excess of that in year 1820, to the values of those quantities in Julian year 2019. The analysis here is limited to impacts of climate change that are small enough to report them as percentage changes in extrapolations of historical estimates of what GDP would be without accounting for influences of anthropogenic climate change. Extrapolations of regional GDP are regional populations P_r times extrapolations of per capita GDPs. How the extrapolations of population and per capita GDP were made is described below in Appendix C.

4.2. **No Deals Results.** Figure 3 shows the evolution of productivity impacts for all 16 regions. For regions that have a positive maximum impact after 2023, the years for those maxima are USA (2034), CAN (2045), JPK (2081), and ANZ (2090).

Some insights into the types of impacts that are important in different regions are provided in Figures 4 and 5 and Table 5. Plotted in Figures 4 and 5a are climate change productivity impacts divided by $\omega = 0.675$, in units of percent. Those curves are computed from values and sums of the functions f_r^{XY} defined in Equations 2.1 and 2.2. In the long-term limit, per Equations C.2 and C.3.those curves approach percentages of incremental per capita GDP defined by Equation C.2 and plotted in Figure 5b. To allow rounding to integers, what are listed in Table 4 are percentage changes from 2019 to 2060 of those of those percent impacts. As evident in Figure 4, including the impact of increasing temperature on water supply increases calculated productivity for the CHI region. Also, for CHI the impact of CO_2 fertilization (primarily on agriculture) overshadows ventilation costs and coral reef damage.

For the Small Island States (SIS) region, the fraction of total land area lost annually to rising sea level is much larger than for other regions. This accounts for the SIS region developing the third most negative fractional GDP impact in the bottom right graph in Figure 3. That overall regional impact on productivity for the SIS region is relentless and broadly geographically distributed. Its calculated value here is much larger than that from the geographically more limited scope of episodic SIS storm damage.

For the most of Africa that composes the SSA region, the economic impact of regional warming on diseases initially dominates all other types of impact together. This is evident from the size of the difference between the solid and dashed curves in Figure 5. Next most important is the net cost of space heating and cooling. That cost for the SSA region is fully dominated by costs of cooling (or economic impacts of incurred without space cooling as temperature rises).

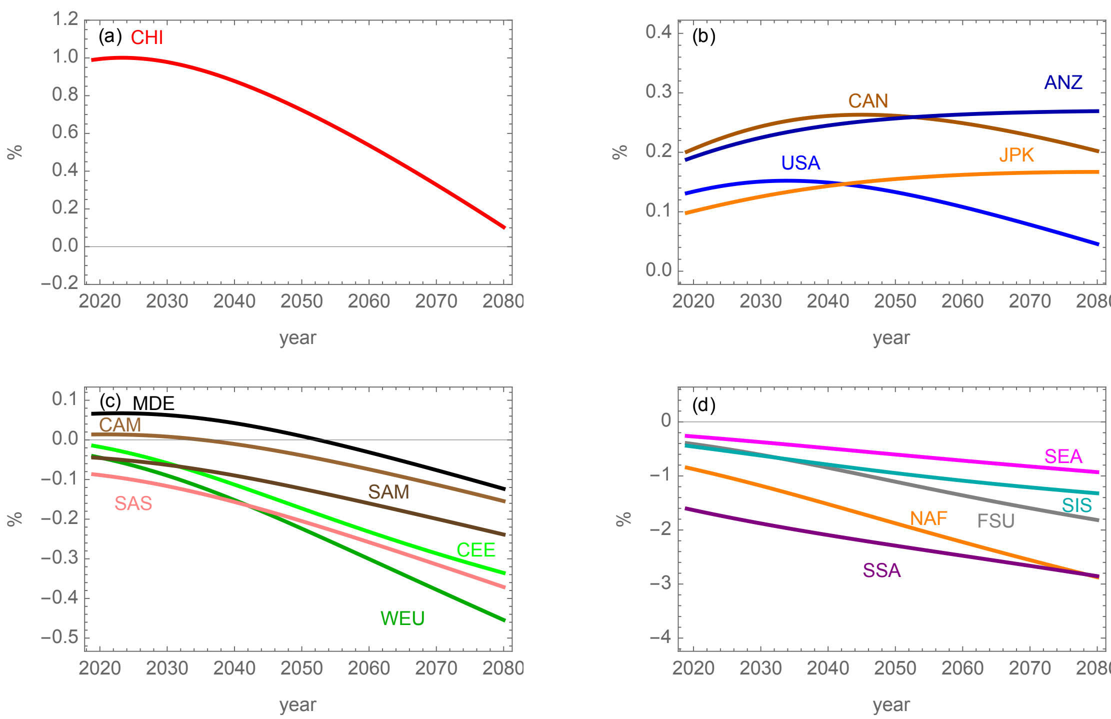

Figure 3. Evolution of percentage impacts on productivity from the trajectories of τ and $<CO_2>$ shown in Figure 2.

For the SSA region, rising $<CO_2>$ makes the next most important contribution to reducing productivity. This is because the economic impact of exposure to humans of higher $<CO_2>$ (or the cost of limiting that exposure in enclosed spaces) is reckoned as the same per person in purchasing power parity, while a much larger total number of people is required for a given amount of GDP in a region like SSA with much lower incremental per capita GDP (c.f. lowest curve in the plots of incremental per capita GDP in Figure 5).

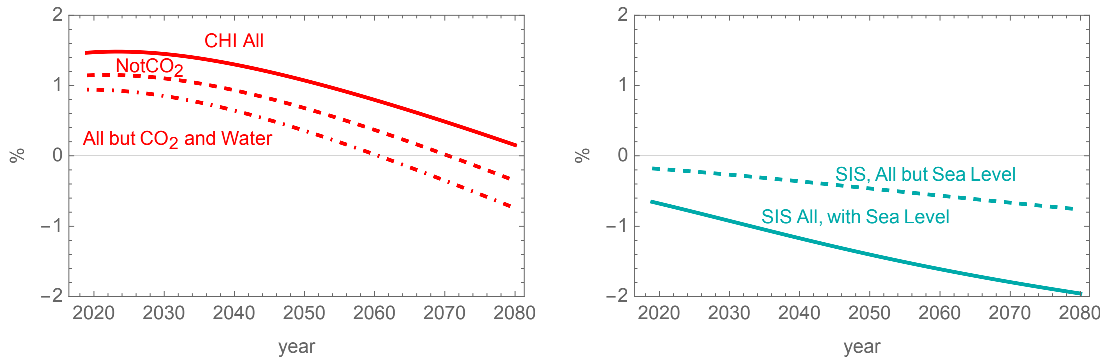

Figure 4. Evolution (a, left) of productivity impacts divided by $\omega = 0.675$ for the CHI region for total impacts (solid curve), total impact less effects of $<CO_2>$ increase (dot-dashed curve), and total impact less effects of $<CO_2>$ increase and effects on water supply (dashed curve); and (b, right) on the Small Island States (SIS) region for total impact (solid curve) and all impacts except from sea level increase (dashed curve).

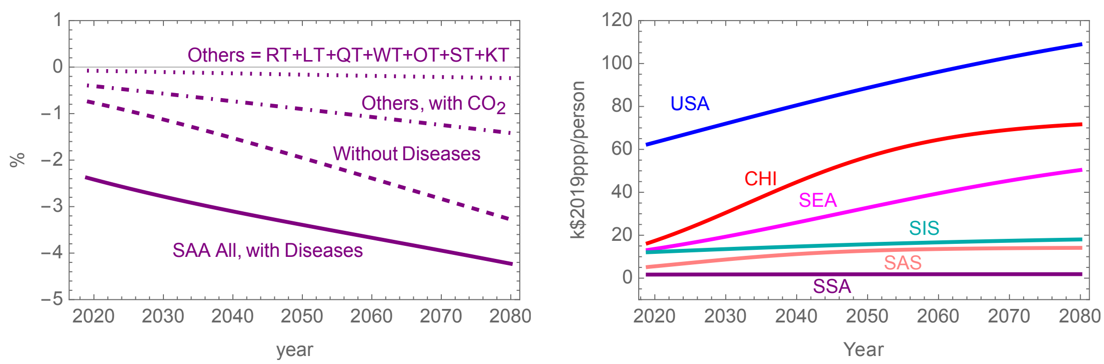

Figure 5. (a, left) Evolution productivity impacts divided by $\omega = 0.675$ for the SSA part of Africa for total impact (solid curve), all but from diseases (dashed curve), all but diseases and heating and cooling (dot-dashed curve), and all but diseases, heating and cooling, and $<CO_2>$ increase (dotted curve); (b, right) evolution for six regions of background (without climate change impacts) increment of per capita GDP over constants b_0 in Table C1.

Table 5 lists the portions from different impacts of the total absolute value of productivity **decline** from 2019 to 2060. These are expressed in percentages of the total percentage decline from 2019 for each region. Since Table 5 lists percentage of a decline, negative entries indicate impacts that tend to counter that decline. For the six regions with entries in Table 5, impacts of temperature increase on space heating and cooling costs are dominated by cooling by 2060, giving positive numbers for the associated declines in productivity. Except for the SSA and SIS regions, the CO_2 fertilization of agriculture results in net positive contribution to productivity, and thus associated negative numbers for the percentages of decline in productivity listed in Table 5. For the SSA region (non-Mediterranean Africa), direct effects of human exposure to carbon dioxide account (or costs of ventilation systems to limit that exposure) account for a 64% contribution to the percentage productivity decline listed in Table 5, overwhelming CO_2 fertilization of agriculture. For the SIS

(Small Island States) that contribution is 8%, with the addition of another 10% due loss of coral reefs. Those effects together are sufficient to account for the positive number of 5% listed in Table 5.

Table 5. % of percentage productivity **Decline** from 2019 to 2060

Impact	USA	SAS	SEA	CHI	SSA	SIS
ag/forestry, except $<CO_2>$	34	6	1	8	-3	-0
$<CO_2>$, sum of all impacts	-131	-5	-5	-16	44	5
Water	87	16	14	-22	11	6
Space Heat and Cool	102	86	81	129	76	27
Sea Level	1	2	10	0	0	60
Diseases	-22	-8	-1	-0	-23	-5
Storms	30	1	0	0	0	5

In 2019, calculated impacts of temperature increase on the contribution of agriculture to productivity are all positive. The corresponding terms for forestry are small enough to have no impact of interest despite being included for completeness when calculating the numbers in Table 5. Except for the region that includes China, by 2060, the terms quadratic in temperature for agriculture summed with the linear terms make only minor contributions to changes in overall productivity from 2019 to 2060. Including CO_2 fertilization of agriculture leads to increases in productivity, except for non-Mediterranean Africa (SSA) where direct effects on human productivity have already made an impact by 2060.

The CHI region's impact of temperature on the cost of water supply is the only region for water to substantially tend to counter a decline in productivity from 2019 to 2060. There is also particular influence on productivity from temperature impacts on water resources that is a dominant negative one for the Former Soviet Union (FSU) region.

Impacts of sea level increase are listed separately in Table 5 to emphasize their importance for the small island states (SIS) region. That is the only region for which impacts from sea level increase dominate all other productivity changes by 2060.

If included separately in Table 5, the cooling and heating impacts on productivity decline for the USA region would respectively be 652% and -550% of the total impacts, mostly canceling to give the 102% entry in Table 5. For the USA case, impacts on disease (in that case diarrhea) and storm damage do show up as double digits in Table 6, but at an order of magnitude lower level than for cooling. As time moves on beyond 2060, cooling costs increase quadratically while storm damages and disease costs scale linearly with temperature, with additional decline in disease impacts with technological progress on timescales of at most 30 years. The USA cooling costs thus evolve to be even more dominant beyond 2060. The percentage contributions of disease impacts to the reduction of productivity from 2019 to 2060 are slightly negative for the SAS, SEA, and CHI, in view of global technological progress and medical progress correlated with increasing per capita GDP outpacing the tendency of temperature rise to increase economic impacts of disease. As illustrated in Fig. 5a, disease impacts on the SSA region are still important in 2060 and beyond; but due to diffusion of global progress on disease control their relative importance compared to other climate change impacts is declining.

4.3. **Mitigation, Transfers, and SRM.** Tables 6 and 7 compare productivity impacts of climate change at the end of the twenty-first century to the No Deals case described above to two illustrative examples. For the first of these, the CHI region pays for the direct cost of enough stratospheric sulfur injection to limit global average temperature to $\tau = 0.56°C$ by 2100. For the second example, each region limits its carbon emissions to a multiple of extrapolated values without new policy implementation. As an incentive to do this, three regions cooperate to pay for some costs of carbon emissions limitations by eight other regions.

Table 6. Productivity % Impacts in 2100

	No Deals	$\tau \to 0.56°$C	$\tau \to 0.56°$C
Region	D	D	D_S
USA	-0.02	0.04	0
CAN	0.14	-0.02	0
WEU	-0.61	0.14	0
JPK	0.16	0.05	0
ANZ	0.27	0.18	0
CEE	-0.42	0.05	0
FSU	-2.20	0.07	0
MDE	-0.22	0.01	0
CAM	-0.24	0.26	0
SAM	-0.32	0.20	0
SAS	-0.28	-0.05	0
SEA	-1.13	0.11	0
CHI	-0.38	0.17	-0.04
NFA	-3.47	0.15	0
SSA	-3.27	-0.93	0
SIS	-1.51	0.16	0

For the example with results listed in Table 6, input parameters were g_s ={-2.9,2037,4,2067,4,2031,2} with g_{s1} dimensionless and the rest in years, $F_{\rm type} = 15.545$ W/m^2, $S_{\rm ref} = 23.695$ MtonneS/yr, and $c_{\rm SRM} = 0.0046$ T\$2019ppp/TtonneS. The values used for $F_{\rm type}$ and $S_{\rm ref} = 23.695$ are from a fits to global circulation model calculations by Laasko et al. [33]. That value of $S_{\rm ref}$ is the average of two nearly identical estimates from fits to sets of calculations using two different microphysics models, of which the other gives a substantially different value of $F_{\rm type} = 6.2693$ W/m^2. The estimate for $c_{\rm SRM}$ is based on work by Smith [10].

Table 7 lists the total regional productivity impacts D in Julian year 2100 for the indicated transfer payment fractions f_{Tr}. The productivity impacts $D_{\rm pay}$ for making transfer payments and the productivity impacts D_E from implementing carbon emissions limitations, net of any transfer payments received, are also listed in Table 7. For the example with results listed in Table 7, historically extrapolated anthropogenic atmospheric carbon emissions were multiplied by 1 for the

JPK region. For all of the other regions, that multiple was given by

$$
\begin{aligned}
(4.1)\qquad e_{23} &= e^{g_2}/e^{g_3} \\
(4.2)\qquad f_{23} &= 1/e_{23} \\
(4.3)\qquad e_{45} &= e^{g_4}/e^{g_5} \\
(4.4)\qquad f_{45} &= 1/e_{45} \\
(4.5)\qquad e_{y3} &= e^{(t-t_1)/g_3} \\
(4.6)\qquad e_{y5} &= e^{(t-t_1)/g_5} \\
(4.7)\qquad f_{p1} &= (1+f_{23})g_3 \ln[1+e_{23}] - (1+f_{45})g_5 \ln[1+e_{45}] \\
(4.8)\qquad f_p &= (f_{45}-f_{23})(t-t_1) + (1+f_{23})g_3 \ln[e_{y3}+e_{23}] - (1+f_{45})g_5 \ln[e_{y5}+e_{45}] \\
(4.9)\qquad f_g &= 1 - u_{23}(t_s, b_{s3}) + u_{23}(t_s, b_{s3})(1 - g_1 + g_1 f_p/f_{p1})
\end{aligned}
$$

with g_1 ={0.211,36,8,10,4}. That function decreases from 1 to an asymptotic limit of 0.779, getting {1,10,50,90,99} % of the way to that limit in years {2028, 2032, 2044, 2063, 2087}. (With the other parameters the same and g_1 chosen to give a limit below 0.779 some regions have lower computed welfare when part of the welfare of other regions in empathetically included in those computations using formulas described in a companion report [11].)

Table 7. Global Partial Green Deal f_{pay} Fractions and Productivity % Impacts in 2100

Region	f_{Tr}	D	D_{pay}	D_E
USA	0.57	-0.35	-0.11	-0.26
CAN	0	0.02	0	-0.15
WEU	-0.12	-0.65	0	-0.13
JPK	-0.63	0.11	0	-0.06
ANZ	0	0.10	0	-0.15
CEE	-0.31	-0.46	0	-0.11
FSU	0	-2.01	0	-0.15
MDE	-0.63	-0.22	0	-0.06
CAM	-0.76	-0.23	0	-0.04
SAM	-0.73	-0.31	0	-0.04
SAS	-0.70	-0.46	0	-0.05
SEA	0	-1.15	0	-0.15
CHI	0.40	-0.39	-0.05	-0.20
NFA	0.03	-3.27	-0.03	-0.18
SSA	-1.00	-2.81	0	0
SIS	-0.48	-1.44	0	-0.08

The numbers in Tables 6 and 7 provide only a snapshot of extrapolated productivity impacts at a particular time. Influence on overall human welfare depend on the temporal evolution of such impacts, of which examples are shown in Figure 3. A companion report provides formulas for quantifying those influences [11].

4.4. **Discussion.** In view of large uncertainties in the values of many parameters used here, the purpose of this report, as noted above, is to highlight interesting questions, not to provide definitive answers. Outstanding amongst these concerns disease in Africa. Given its large and still rapidly growing population and a comparatively low per capita GDP, the prevalence of preventable disease in Africa is one of the world's prevailing impediments to improving overall global human welfare, even without exacerbation from accompanying increases in regional average temperature. This suggests paying attention to what would be the impact of focusing more attention on adaptation to deal with this underlying problem.

Concerning the analysis reported here, the respectively strong positive and negative influences on productivity of increases in temperature on water supplies for the CHI and FSU regions may be indicative of a need for more attention on how to better address those in an economic impact model of moderate complexity.

Above in Figure 3, all but two sixteen regions have further impacts of No Deals climate change on productivity after Julian year 2045 becoming less economically favorable. (The exceptions are the JPK and ANZ regions, where much of the population lives in temperate regions where land temperatures are moderate by proximity to the sea.) In view of estimates of the comparatively small direct cost of limiting further temperature increase via anthropogenic stratospheric sulfur injection [10], can alternative approaches to limiting radiative forcing overcome impediments to funding and implementing alternatives that include much more substantial limits on global greenhouse gas emissions? This is by no means a new question, but models such as the one described here provide an option of a readily reproducible tool for investigating such questions.

Appendix A. Geographic Regions and GDP and Population Parameter Tables

A.1. **Geographic Regions.** Table A1 lists International Standards Organization codes for the components of sixteen geographic regions. Table A.2 describes some features of the regional compositions. As in the FUND 3.9 documentation, the Taiwan province of China is included with the Southeast Asia (SEA) region, and Puerto Rico is included with the Small Island States (SIS). Unlike for FUND 3.9, the Baltic states of Estonia, Latvia, and Lithuania are included with Central and Eastern Europe (CEE) rather than with the Former Soviet Union (FSU). Table A.3 writes out the names of the components of the SIS region.

Table A1. Region Components

Region	ISO	Code										
USA	USA											
CAN	CAN											
WEU	AND	AUT	BEL	CHA	CYP	DNK	FLK	FRO	FIN	FRA	DEU	GIB
	GRC	GRL	ISL	IRL	IMN	ITA	LIE	LUX	MLT	MCO	NLD	NOR
	PRT	SMR	ESP	SWE	CHE	GBR						
JPK	JPN	KOR										
ANZ	AUS	NZL	NIU	TKL								
CEE	ALB	BIH	BGR	HRV	CZE	EST	HUN	LVA	LTU	MKD	MNE	POL
	SRB	SVK	SVN									
FSU	ARM	AZE	BLR	GEO	KAZ	KGZ	MDA	RUS	TJK	UKR	UZB	
MDE	BHR	IRN	IRQ	ISR	JOR	KWT	LBN	OMN	PSE	QAT	SAU	SYR
	TUR	ARE										
CAM	BLZ	CRI	SLV	GTM	HND	MEX	NIC	PAN				
SAM	ARG	BOL	BRA	CHL	COL	ECU	GUF	GUY	PRY	PER	SUR	URY
	VEN											
SAS	AFG	BGD	BTN	IND	NPL	PAK	LKA					
SEA	BRN	KHM	IDN	LAO	MYS	MMR	PNG	PHL	SGP	TWN	THA	TLS
	VNM											
CHI	CHN	HKG	MAC	PRK	MNG							
NAF	DZA	EGY	LBY	MAR	TUN	ESH						
SSA	AGO	BEN	BWA	BFA	BDI	CMR	CPV	CAF	TCD	COG	COD	CIV
	DJI	GNQ	ERI	ETH	GAB	GMB	GHA	GIN	GNB	KEN	LSO	LBR
	MDG	MWI	MLI	MRT	MOZ	NAM	NER	NGA	RWA	SEN	SLE	SOM
	ZAF	SSD	SDN	SWZ	TZA	TGO	UGA	ZMB	ZWE			
SIS	ASM	AIA	ATG	ABW	BHS	BRB	BMU	BES	VGB	CYM	COM	COK
	DJI	GNQ	ERI	ETH	GAB	ETH	GAB	GMB	GHA	GIN	GNB	KEN
	CUB	CUW	DMA	DOM	FJI	PYF	GRD	GLP	GUM	HTI	JAM	KIR
	MDV	MHL	MTQ	MUS	FSM	NRU	NCL	MNP	PLW	PRI	REU	
	SHN	KNA	LCA	VCT	BLM	MAF	WSM	STP	SYC	SXM	SLB	TON
	TTO	TCA	TUV	VUT	VIR	WLF						

Table A2. Region Names and Some Constituents

Region	Name	
USA	USA	
CAN	Canada	
WEU	Western Europe	with Greenland (GRL)
JPK	Japan and South Korea	
ANZ	Australia and New Zealand	with Niue (NIU), Tokelau (TKL)
CEE	Central and Eastern Europe	including Baltics
FSU	Former Soviet Union	without Baltics
MDE	Middle East	with Turkey (TUR)
CAM	Central America	
SAM	South America	
SAS	South Asia	with Afghanistan (AFG)
SEA	Southeast Asia	with Papua New Guinea (PNG), Philippines (PHL), Taiwan (TWN)
CHI	China plus	without Taiwan Province, with North Korea (PRK), Mongolia (MNG)
NAF	North Africa	Mediterranean + Western Sahara (ESH)
SSA	Sub-Saharan Africa	with Cape Verde (CPV)

Table A3. SIS, Small Island States

American Samoa, Anguilla, Antigua and Barbuda, Aruba, Bahamas, Barbados, Bermuda, Bonaire Sint Eustatius and Saba, British Virgin Islands, Cayman Islands, Comoros, Cook Islands, Cuba, Curaçao, Dominica, Dominican Republic, Fiji, Federated States of Micronesia, French Polynesia, Grenada, Guadeloupe, Guam, Haiti, Jamaica, Kiribati, Maldives, Marshall Islands, Martinique, Mauritius, Montserrat, Nauru, New Caledonia, Northern Mariana Islands, Palau, Puerto Rico, Réunion, Saint Barthélemy, Saint Helena, Saint Kitts and Nevis, Saint Lucia, Saint Pierre and Miquelon, Saint Vincent and the Grenadines, Saint Martin (French Part), Samoa, São Tomé and Príncipe, Seychelles, Sint Maarten (Dutch Part), Tonga, Trinidad and Tobago, Tuvalu, United States Virgin Islands, Vanuatu, Wallis and Futuna Islands

Appendix B. Calculation of Impact Coefficients c_r^{XY} in Julian Year 2019

This appendix contains tables of parameter values used to calculate the entries for c_r^{XY} in Table 1 by evaluating, for Julian year 2019, the formulas given below. The formulas here for F_r^{XY} are for fractional impacts from climate change on GDP and have values of zero in 1990. When evaluated at $t_1 = 2019$ to calculate the entries for c_r^{XY} in Table 4 of Section 2, the results are multiplied by 100 because those entries for c_r^{XY} are percents. The formulas f_r^{XY} in the main text, which have leading coefficients c_r^{XY}, are then multiplied by $\omega = 0.675$ to get formulas for percentage changes in productivity, as described immediately after Table C.2 below.

This appendix also contains pointers to FUND 3.9 tables of additional region-dependent parameters [8]. For example, (RT 2) points to regional temperature conversion factors in column 2 of Table RT in [8]. The function of this appendix is to provide information aimed at making the calculations used for the present work capable of being independently reproduced or modified. As such, there is minimal additional discussion of the rationale, beyond what is included above in Section 3.

B.1. **Agriculture.** The agricultural fractions of GDP are

$$F_r^{AE} = c_r^{AE}(y_r/y_{1r})^{\zeta_r} \tag{B.1}$$

Tables 2 and B1 list values of the region-dependent parameters in this equation. Agricultural production values in “2014–2016” International dollars from 1961–2019 were multiplied by the 2019 to 2015 U.S. consumer price ratio [34]. Early missing values for the Marshall Islands and the Federated States of Micronesia were filled in with the first temporally available entry. Late missing entries for French Guyana, Guadeloupe, Martinique, and Réunion were filled in with the last temporally available entry, and the those amounts were subtracted from entries for France. Early missing entries for Palestine were the corresponding entry for Israel multiplied by the first temporally available ratio of Palestine/(Israel+Palestine). Early missing entries for Estonia, Latvia, and Lithuania Baltic countries were similarly filled in using earliest available ratios for those countries to the total for what had been in the USSR. The FSU total for those earlier years was then the USSR entries less the totals for the Baltics. Fractions of GDP for each region were summed agricultural production values divided by the regionally summed GDP’s from the data sources discussed in a companion report [11].

Table B1. Agriculture Fraction vs. per Capita GDP Coefficients, c_r^{AE}

USA	CAN	WEU	JPK	ANZ	CEE	FSU	MDE
.01873	.02524	.01467	.00599	.04323	.02544	.03791	.01923
CAM	SAM	SAS	SEA	CHI	NAF	SSA	SIS
.02672	.05642	.04809	.03274	.04876	.03184	.09593	.02086

Impacts associated with the rate of change of global temperature are

$$F_r^{AR} = F_r^{AE}\rho_{AR}(\alpha_r^{AR}/100)(R_r^T)^2(\tau'^{\,2} - {\tau_0}'^{\,2})/\delta_{AR}^2 \tag{B.2}$$

Table B2 lists the values of ρ_{AR} and δ_{AR}. Pointers are α_r^{AR} (A 2), and R_r^T (RT 2). (These numbers are fractions, not percents.) The units of $(\alpha_r^{AR}/100)$ are 1/yr. A denominator of 100 is included in $(\alpha_r^{AR}/100)$, because the values in (A 2) are in percent.

Table B2. Global Constants

Symbol	Value	Units
τ_1	1.309	°C
τ_1'	0.024	°C/yr
$< CO_2 >_1$	410	ppm
ρ_{AR}	10	1
δ_{AR}	0.04	°C/yr
$< CO_2 >_{\text{pre}}$	275	ppm
γ_{FC}	0.44	1
α_{VC}	0.148	(\$2019/yr)/ppm
R_{OT}	6.3	1
V_{OC}	0.225	T\$2019/(Mm)^2
V_K	200	1
V_M	0.8	1
C_T	13.6	°C
α_{MD}	0.0794	1/°C
α_{DF}	0.3534	1/°C
α_{SM}	-0.1149	1/°C
γ_{ST}	3	°C/yr
δ_{ST}	0.04	°C

Impacts associated with two different powers of global average temperature are

(B.3) $$F_r^{AL} = F_r^{AE} \delta_r^{AL} R_r^T T$$

(B.4) $$F_r^{AQ} = F_r^{AQ} \delta_r^{AQ} (R_r^T T)^2$$

Pointers are δ_r^{AL} (A 4) and δ_r^{AQ} (A 6).

Impacts from CO_2 fertilization of agriculture are, with γ_r^{AC} in (A 8) in percent,

(B.5) $$F_r^{AC} = F_r^{AE} (\gamma_r^{AC}/100) \ln(< CO_2 > / < CO_2 >_{\text{pre}})$$

The value of $< CO_2 >_{\text{pre}}$ listed in Table B2 is a reference preindustrial value of $< CO_2 >$ used in the FUND 3.9 documentation. Values of τ_1, τ_1', and $< CO_2 >_1$ needed for calculating $T_1 = \tau_1 - \tau_0 = 0.594$°C and F_r^{XY} at time t_1 are also listed in Table B2.

B.2. **Forestry.** Impacts from temperature effects on forestry are, with pointer α_r^F (EFW 2),

(B.6) $$F_r^{FT} = (y_r/y_{0r})^{\epsilon_{FT}} (0.5\, \alpha_r^F) T$$

impacts from $< CO_2 >$ fertilization of forestry are

(B.7) $$F_r^{FC} = (y_r/y_{0r})^{\epsilon_{FC}} (0.5\, \alpha_r^F \gamma_{FC}) \ln(< CO_2 > / < CO_2 >_{\text{pre}})$$

The value of γ_{FC} is listed in Table B2. Elasticities $\epsilon_{FT} = \epsilon_{FC}$ are in Table 1 of Section 2. The FUND 3.9 documentation writes the forestry income elasticity effects as proportional to $(1/y_r)^\epsilon$ with $\epsilon = 0.31$ having a positive value for ϵ, so elasticity proportional to a power of y_r as above in Section 2 has $\epsilon_{FT} = \epsilon_{FC} = -0.31$.

B.3. **Water.** Impacts from temperature effects on water supply, with pointer α_r^{WT} (EFW 4), are

$$F_r^{WT} = (y_r/y_{0r})^{\epsilon_{WT}}(P_r/P_{0r})^{\epsilon_{WT}} 0.995^{t-2000}\alpha_r^{WT} T \tag{B.8}$$

With the value of $t_{1/2}^{WT}$ listed in Section 2, Table 1, the technology improvement factor is approximated in Section 2 as being proportional to $2^{-\nu_{WT}(t-t_1)/t_{1/2}^{WT}}$. The FUND 3.9 documentation estimates the impact on GDP from temperature effects on water sources to be proportional to GDP to the 0.85 power. Dividing by total GDP to get the fractional impact gives $\epsilon_{WT} = 0.85 - 1 = -0.15$ in Table 1 of Section 2. Formulas and parameters for population, P_r, are in Appendix C below.

B.4. **Space Heating and Cooling.** Impacts from temperature effects on space heating, with pointer α_r^{HT} (EFW 6), are

$$F_r^{HT} = (y_r/y_{0r})^{\epsilon_{HT}}\alpha_r^{HT}\text{ArcTan}(T)/\text{ArcTan}(1) \tag{B.9}$$

The α_r^{HT} space heating coefficient for the Middle East in FUND 3.9 table EFW for the Middle East (MDE) was 4.8 times as large as that for the USA. For the regions where it reduced the FUND 3.9 impacts (MDE, CAM, SAM, SAS, SEA, and SIS), the coefficients for the ArcTan$(\tau - \tau_0)$ function were here set equal to the USA region values times ratios of years 1997–2013 averages of U.S. National Weather Service heat index heating degree days [35] to that for the USA region. Those numbers were weighted by year 2005 population for all countries in each region for which heating degree days entries were listed.

Impacts from temperature effects on space cooling are $(y_r/y_{0r})^{\epsilon_{CT}}\alpha_r^{CT}(\tau^2 - \tau_0^2)$, with pointer α_r^{CT} (EFW 8). To avoid imaginary numbers for temperatures lower than the 1990 value, this formula has that effect proportional to $\tau^2 - \tau_0^2$, where τ_0 is the year 1990 temperature. This model matches the FUND 3.9 model for temperatures in 1990, 2019, and when $\tau = 4.19$ °C.

The FUND 3.9 documentation has the impacts on GDP from temperature effects on space heating and cooling both proportional to $y_r^{0.8}P_r$. Dividing by total GDP to get a fractional impact gives $\epsilon_{HT} = \epsilon_{CT} = 0.8 - 1 = -0.2$ in Table 1 of Section 2.

B.5. **Ventilation.** Impacts of CO_2 effects on human cognition give

$$F_r^{VC} = -(1000\, y_r)^{-1}\alpha_{VC}(< CO_2 > - < CO_2 >_0) \tag{B.10}$$

The value of $\alpha_{VC} = C_{VC}V_{VC}\rho_{VC}$ listed in Table B2 is is computed from three parameters. The cost per tonne of CO_2 scrubbing in UDS2019 of $C_{VC} = 600(225.7/229.4)$ is an estimate of the cost published in 2009 [23] times a 2019 to 2009 U.S. consumer price index [34] ratio. The ventilation rate in liters per year for each person is $V_{VC} = 11.7 * 0.3 * (3600 * 24 * 365.25)$, with occupancy space [25] of 11.7 m^2/person and ventilation rate of 0.3(l/s)/m^2 [24] converted to (l/yr)/m^2 by multiplying by the number of seconds in a year. The number of tonnes of CO_2 per ppm CO_2 is $\rho_{VC} = 10^{-6}(44 * 10^{-6})/22.4$. The factor of 1000 is included before y_r in the expression $(1000 y_{1r})^{-1}$ because the values of y_r are computed using parameters in Table C1 that have units of 1000s of dollars/person. The 0.3(l/s)/m^2 standard for an indoor CO_2 concentration limit of 1000 ppm is used as a proxy at the time of standards setting for other less easily measured indoor pollutants. So that ventilation rate is used here even for situations where outdoor $< CO_2 >$ changes substantially over time.

B.6. **Sea Level.** Impacts from sea level change are estimated as $(\text{km})^2$/yr of dry land loss times value per km^2, divided by GDP. The formula for this is

$$F_r^{OT} = -R_{OT}(\delta_r^{OT}/(10^6 A_r^{OT}))dH_m^{1+\sigma_r}/dt \tag{B.11}$$

where $H_m = H/(1\ m)$. The expansion of the time derivative $dH^{1+\sigma_r}/dt = (1 + \sigma_r)H^{\sigma_r}dH/dt$ with $dH/dt = dS/dt = a_S(\tau - \tau_S)$ is used to get the results for c_r^{OT} in Table 1 of Section 2.

The value of $R_{OT} = 6.3$ listed in Table B2 is the ratio 4/0.635, rounded from 6.299, of parameters denoted in the Fund 3.9 documentation as ϕ=4 M/$(\text{km})^2$ and YA_0=0.635 M/$(\text{km})^2$. The parameters

δ_r^{OT} (pointer SLR 2), are $(\mathrm{km})^2$ of cumulative land area losses per unit of $(S/(1\,m))^{\sigma_r}$, where $S/(1\,m)$ denotes sea level increase since 1750 (with 1 m in the denominator to make $S_r/(1\,m)$ dimensionless). The exponents σ_r listed in Table 3 in Section 2 are computed from FUND 3.9 $(1+\sigma_r)$ values (SLR 3). Also in Section 2 are formulas for computing S as a function of time. Total regional land areas A_r^{OT} in $(\mathrm{Mm})^2$ are listed in Table B3 [36]. The factor of 10^6 in front of A_r^{OT} in the above equation for F_r^{OT} converts these numbers to $(\mathrm{km})^2$.

Table B3. Total Regional Land Areas A_r^{OT} in $(\mathrm{Mm})^2$

USA	CAN	WEU	JPK	ANZ	CEE	FSU	MDE
9.640	9.971	6.349	0.477	8.012	0.855	22.308	6.283
CAM	SAM	SAS	SEA	CHI	NAF	SSA	SIS
2.480	17.820	5.139	4.958	11.283	6.019	24.285	0.321

B.7. **Coral Reef Loss.** Fractional impacts from coral reef loss are

$$F_r^{OC} = -V_{OC} A_r^{OC} (R - R_0)/Y_{1r} \tag{B.12}$$

Here the entry for $V_{OC} = (255.7/177.2)0.177$ T\$2019 per $(\mathrm{Mm})^2$ of coral reefs as listed in Table B2 is inflation-adjusted from year 2000 to year 2019 [34], A_r^{OC} are summed coral reef areas listed in Table B4 for the regions [16], $Y_{1r} = y_{1r} P_{1r}$ are regional GDP values in T\$2019, and the formula for the cumulative coral reef fractional loss R is given in Section 2. For sea level changes and coral reef loss, coastal dry land and coral reef values are considered to be luxury goods valued in inflation-adjusted U.S. dollars with no region-dependent purchasing power parity adjustments.

Table B4. Preindustrial Coral Reef Areas A_r^{OC} in $(\mathrm{Mm})^2$

USA	CAN	WEU	JPK	ANZ	CEE	FSU	MDE
0.00143	0	0	0.00290	0.04896	0	0	0.01122
CAM	SAM	SAS	SEA	CHI	NAF	SSA	SIS
0.005040	0.00354	0.00657	0.011654	0.00151	0.00380	0.01692	0.06964

B.8. **Diseases and Storm Damage.** The fractional impacts from mortality and morbidity caused by diarrhea are respectively

$$F_r^{DT} = -(y_r/y_{0r})^{\epsilon_{DT}} 2^{-\nu_{DT}(t-2000)/t_{1/2}^{DT}} V_K (\mu_r^{DT}/1000) \eta_{DT} R_r^T T/C_T \tag{B.13}$$

$$F_r^{MT} = -(y_r/y_{0r})^{\epsilon_{MT}} 2^{-\nu_{MT}(t-2000)} V_M (\mu_r^{MT}/1000) \eta_{MT} R_r^T T/C_T \tag{B.14}$$

The value of $C_T = 13.6$ [37] is an estimate of the preindustrial global average in °C (i.e. absolute temperature in Kelvin less 273.13). The expression $(1+\delta_{DT}\tau/C_T)^{\eta_{DT}} - (1+\delta_{DT}\tau_0 C_T)^{\eta_{DT}}$ that would follow from using the formula in the FUND 3.9 documentation has been replaced by expansions through first order in τ/C_T and τ_0/C_T for simplicity, and similarly for F_r^{MT}.

The parameters $V_K = 200$ and $V_M = 0.8$, from the FUND 3.9 documentation and listed in Table B2, are ratios. Those ratios are cost per person of death, or the onset of morbidity form diarrhea, divided by per capita GDP. The parameters μ_r^{DT} (HD 3) and μ_r^{MT} (HD 4) are respectively the corresponding increases of mortality and morbidity per °C of regional temperature increase. Values for η_{DT} and η_{MT} are listed in Table B2. Values for ϵ_{DT}, ϵ_{MT} and $\nu_{DT} = \nu_{MT}$ are listed in Table 1 of Section 2.

The fractional impacts from mortality due to vector-borne disease are

$$F_r^{VT} = -(y_r/y_{0r})^{\epsilon_{VT}} 2^{-\nu_{VT}(t-2000)} V_K 10^{-6} (\mu_r^{MD}\alpha_{MD} + \mu_r^{DF}\alpha_{DF} + \mu_r^{SM}\alpha_{SM}) R_r^T T \tag{B.15}$$

Here μ_r^{MD} (HV 2), μ_r^{DF}, (HV 4), and μ_r^{SM} (HV 6) are respectively base level annual mortality rates (per million people, hence the factor of 10^{-6}) respectively from malaria, dengue fever, and schistosomiasis. Corresponding changes in those mortalities per °C of regional temperature increase, α_{MD}, α_{DF}, and α_{SM} from Table HV of [8], are listed in Table B2. Values of ϵ_{VT} and ν_{VT} are listed in Table 1 of Section 2.

Fractional impacts due to property damage from storms are

$$F_r^{ST} = F_r^{PS} + F_r^{PE} \tag{B.16}$$

where

$$F_r^{PS} = -(y_r/y_{0r})^{\epsilon_{ST}} \alpha_r^{PS} \delta_{ST} \gamma_{ST} T \tag{B.17}$$

and

$$f_r^{PE} = -(y_{r/}y_{0r})^{\epsilon_{ST}} \alpha_r^{PE} \delta_r^{PE} R_{TC} T \tag{B.18}$$

with

$$R_{TC} = \frac{((< \mathrm{CO}_2 >_1 / < \mathrm{CO}_2 >_{\mathrm{pre}}) - 1)}{T_1} \tag{B.19}$$

Here, α_r^{PS} (TS 2) and α_r^{PE} (ETS 2) are background property damage rates from tropical and extratropical storms respectively. Values for γ_{ST} and δ_{ST} are listed in Table B2. The value of ϵ_{ST} is listed in Table 1 of Section 2. The parameters δ_r^{PE} (ETS 3) are regional sensitivities to extratropical storms from climate change. Conversion from sensitivities to $< CO_2 >$ to sensitivities to global average temperature is done using the ratio R_{TC}.

Fractional impacts due to people being killed by storms are

$$F_r^{KT} = F_r^{KS} + F_r^{KE} \tag{B.20}$$

where

$$F_r^{KS} = -(y_r/y_{0r})^{\epsilon_{KT}} V_K \alpha_r^{KS} \delta_{ST} \gamma_{ST} T \tag{B.21}$$

and

$$F_r^{KE} = -(y_{r/}y_{0r})^{\epsilon_{KT}} V_K 10^{-6} \beta_r^{KE} \delta_r^{PE} R_{TC} T \tag{B.22}$$

Here α_r^{KS} (TS 3) and β_r^{KE} (ETS 4) are background mortality rates from tropical and extratropical storms respectively. (FSU and CAM FUND 3.9 table entries for β_r^{KE} (ETS 4) are identical to five digits but were nevertheless left as is in view of their resulting very small values of c_r^{KE} for both.) Including the factor of 10^{-6} in front of β_r^{KE} assumes that the entries for β_r^{KE} (ETS 4) are per million people, for consistency with other entries in the FUND 3.9 parameter tables. Values for γ_{ST} and δ_{ST} are listed in Table B2. The value of ϵ_{KT} is listed in Table 1 of Section 2.

Appendix C. Population and per Capita GDP

Table C1 lists values for each region of four parameters in the expression B_0+P for total population, where

$$P = B_1/(1 + e^{-(t-B_2)/B_3}) \tag{C.1}$$

Here P is the change in a region's population from 1820. The parameters in the expression for P were determined by a least squares fit to each region's annual population from 1820 to the earlier of 2050 and a twentieth century maximum population in "medium fertility variant" extrapolations from the United Nations [38]. Those extrapolations are interpreted as not accounting for pronatalist and/or immigration trends assumed here to counter a trend towards an increasing fraction of elderly in the population. How estimates back to 1820 are combined with those from the United Nations is described in a companion report [11].

Table C1. Population (Billion) and per Capita GDP (k$US2019ppp) Constants

Symbol	B_0	B_1	B_2	B_3	b_0	b_1	b_2	b_3
Units	Billion	Billion	Julian yr	yr	k$US2019	k$US2019	Julian yr	yr
USA	0.0100	0.4477	1980.33	43.47	2.87	139.15	1999.93	43.97
CAN	0.0008	0.0565	1994.06	40.31	2.52	79.99	1978.99	35.13
WEU	0.1348	0.3183	1935.90	41.51	4.25	59.74	1972.21	24.75
JPK	0.0406	0.1332	1948.88	19.28	1.64	44.93	1973.41	15.40
ANZ	0.0004	0.0538	2011.22	42.73	7.15	83.22	1992.81	31.28
CEE	0.0374	0.0857	1913.99	30.69	2.07	59.74	2007.24	40.28
FSU	0.0538	0.2634	1939.88	35.72	2.35	17.92	1953.36	15.69
MDE	0.0260	0.5338	2009.02	23.77	1.85	29.57	1975.81	29.99
CAM	0.0080	0.2443	1993.45	24.41	1.86	20.49	1961.68	30.24
SAM	0.0099	0.5447	1988.03	27.25	1.34	24.27	1975.47	40.07
SAS	0.2251	2.5368	2004.11	25.83	1.46	14.26	2014.99	12.06
SEA	0.0407	0.9458	1995.90	30.28	1.19	64.06	2031.38	25.42
CHI	0.3881	1.0811	1974.40	16.22	0.61	74.20	2023.41	14.00
NAF	0.0110	0.3804	2018.84	30.47	1.46	42.62	2036.64	48.12
SSA	0.0650	4.6435	2054.55	29.14	0.98	1.90	1941.26	30.88
SIS	0.0046	0.0607	1982.91	30.60	1.41	20.35	1981.77	37.88

Per capita GDP for each region evolves as $b_0 + y$ where

(C.2) $$y = b_1(a/(1+\delta z)^{\alpha})^{1/\omega}$$

with $z = (1 - a)$ [11]. In the approximation of neglecting small impacts of changes in temperature and $<CO_2>$ associated with climate change, productivity evolves in proportion to

(C.3) $$a = 1/(1 + e^{-(t-b_2)/b_3})$$

with different constants for the resulting evolution of y for each region. Here t is time in Julian years. The region dependent constants b_0, b_1, b_2, and b_3 are listed in Table C1. Values of constants in the formula for y are computed as $\delta = (\bar{t}/b_3)\theta/\omega$, with $\omega = 1 - \alpha$, using global values of α, $\bar{t}$, and θ that are also listed in Table C2. A source of those three parameter values is Singer et al. [39]. The data sources and calibration method for the parameters $\{b_0, b_1.b_2, b_3\}$ in Table C1 are described in a companion report [11].

Table C2. Miscellaneous GDP Constants

Symbol	Value	Units	Meaning
$\bar{t}$	7.76	yr	capitalization time
θ	1.345	1	inverse of inter-temporal substitutability of consumption
α	0.325	1	capital fraction of production
$\omega = 1 - \alpha$	0.675	1	labor fraction of production

Note that $d\ln(y)/d\ln a = (1/\omega)(1 + (\delta\alpha/(1 + \delta z))$, with $\alpha = 0.325$. Neglecting the factor $(\delta\alpha/(1 + \delta z))$, as being small compared to uncertainties [8] in estimates of impacts of climate change on incremental per capita GDP, y gives the approximation that small fractional changes in incremental GDP of the economy can be approximated as $(1/\omega)$ times small fractional changes in a, the productivity.

Appendix D. Anthropogenic Atmospheric Carbon Emissions

The formulas and parameters used here for anthropogenic atmospheric carbon emissions in the form of CO_2 (here called "emissions") are as follows. Depletion of global geological fluid fossil fuel resources is assumed to limit future anthropogenic TtonneC/yr emissions of carbon in the form of CO_2 to

$$e_c = f_c e_{\text{ind}} + (1 - f_c) f_s e_{\text{ind}} + e_{\text{land}} \tag{D.1}$$

where $f_s = (1 - a_s) + a_s f_d$, with $a_s = 1/(1 + e^{t - t_c)/t_s}$,

$$f_d = \left(1 + \frac{1 + b_d \text{Max}[U, U_{2019}]}{1 + b_d U_{2019}}\right)^{\beta_f} \tag{D.2}$$

and the coal fraction f_c of industrial emissions e_{ind} and emissions e_{land} are defined elsewhere [12]. Here cumulative emissions U in TtonneC from Julian year 1750 are [12]

$$U = \beta_1\beta_2 + \beta_1\beta_3 \ln[e^{\beta_2/\beta_3} + e^{t/\beta_3}] + \beta_0(t - 1750) \tag{D.3}$$

The values of constants in these expressions are t_c = year 2002, t_2 = 2 yrs, $\beta_0 = -0.000002$ TtonneC/yr, $\beta_1 = 0.015285$ TtonneC/yr, β_2 = year 2002.57, $\beta_3 = 27.82$ yrs, $b_d = 0.68$ TtonneC^{-1}, $\beta_f = -0.35$, and $U_{2019} = 0.44$ TtonneC.

The logistic function a_s is used to avoid a discontinuity in de_c/dt in a transition from an earlier time when technological advances were assumed to make the fluid fossil fuel resource depletion effect too small compared to other market variations to be included, and a later time when that is no longer the case. This avoids a minor computational problem when multiple derivatives of $< CO_2 >$ are used in subsequent work. The maximum value of the function f_d is 1.00066, in year 2016. The was considered to be a negligible difference from the value $f_d = 1$ that was used to calibrate the carbon emissions formula against historical data through 2019 [12]. The temporal rate of change e_c has an inflection point in year 2020, during the COVID pandemic, at which time $f_d = 0.999$. The effects of the COVID on the longer term evolution of $< CO_2 >$, radiative forcing, and global average temperature are considered to be uncertain enough that no attempt is made here to adjust the carbon emissions functions to account for those effects. Except for inclusion of the smoothing function a_s, the formula for e_c and its parameter values is identical to that documented elsewhere [12], as are the methods for integrating a balance equation for the evolution of the atmospheric CO_2 concentration.

References

[1] Singer, C., and L. Matchett, 2016. Climate action gaming experiment: Methods and example results, *Challenges* **6**, 202-228, https://www.mdpi.com/2078-1547/6/2/202, accessed December 1, 2023.

[2] Kompas, T., V. Pham, and T. Che. 2018. The effects of climate change on GDP by country and the global economic gains of complying with the Paris Climate Accord. *Earth's Future* **6**, Issue 8, https:/doi.org/10.1029/2018EF00092.

[3] Stanton, E., F. Ackerman, and S. Kartha. 2009. Inside the integrated assessment models: Four issues in climate economics. *Climate and Development* **1**, 166–184, https://doi.org/10.3763/cdev.2009.0015.

[4] Gillingham, K., W. Nordhaus, D. Anthoff, G. Blanford, V. Bosetti, P. Christensen, H. McJeon, J. Reilly, and P. Sztorc. 2015. Modelling uncertainty in integrated assessment of climate change: A multi-model comparison, MIT Joint Program on the Science and Policy of Climate Change Report 290. https://globalchange.mit.edu/publication/16235, accessed June 5, 2019.

[5] Nordhaus, W. 2010. Economic aspects of global warming in a post-Copenhagen environment. *Proceedings of the National Academy of Sciences* **107**, 11721–11726, https://doi.org/10.1073/pnas.1005985107.

[6] Anthoff, D., and J. Tol. 2014. The climate framework for uncertainty, negotiation and distribution (FUND), technical description, version 3.9, http://www.fund-model.org/versions, accessed May 18, 2019.

[7] Burke, M., S. Hsiang, and E. Miguel. 2015. Global nonlinear effect of temperature on economic production. *Nature* **527**, 235–239, https://doi.org/10.1038/nature15725.

[8] Anthoff, D., and J. Tol. 2014. The climate framework for uncertainty, negotiation and distribution (FUND), tables version 3.9, http://www.fund-model.org/files/documentation/Fund-3-9-Scientific-Tables.pdf, accessed May 18, 2019.

[9] Heutel, G., J. Moreno-Cruz, and S. Shayegh. 2018. Solar geoengineering, uncertainty, and the price of carbon, *Journal of Environmental Economics and Management* **87**, 24–41, https://doi.org/10.1016/j.jeem.2017.11.002.

[10] Smith, W., and G. Wagner. 2018. Stratospheric aerosol injection tactics and costs in the first 15 years of deployment, *Environmental Research Letters* **13**, 124001, https://doi.org/10.1088/1748-9326/aae98d.

[11] Singer, C. 2024. Economic measure of welfare impacts of changes in temperature and atmospheric carbon dioxide concentration. University of Illinois Program in Arms Control and International Security report ACDIS//ACDIS SIN:2.2024. https://ideals.illinois.edu/items/128960, accessed January 25, 2024.

[12] Ding, C., and C. Singer. 2022. Calibration and extrapolation of a simple global carbon balance model. University of Illinois Program in Arms Control and International Security report ACDIS//ACDIS DIN:2.2022, https://acdis.illinois.edu/system/files/2022-08/CAGE22R2Fronted24Jul.pdf, accessed December 1, 2023.

[13] Ding, C., and C. Singer. 2022. Extrapolations of global average temperature, sea level rise, and ocean pH change. University of Illinois Program in Arms Control and International Security report ACDIS//ACDIS DIN:5.2022, https://acdis.illinois.edu/system/files/2022-08/CAGE22R5Fronted24Jul.pdf, accessed December 1, 2023.

[14] Ding, C., and C. Singer. 2022. Global heat balance equation probability distributions and extrapolations. University of Illinois Program in Arms Control and International Security report ACDIS//ACDIS DIN:6.2022, https://acdis.illinois.edu/system/files/2022-08/CAGE22R6Fronted24Jul.pdf, accessed December 1, 2023.

[15] Grinsted, A., J. Moore, and S. Jevrejeva. 2010. Reconstructing sea level from paleo and projected temperatures, 200–2100 AD, *Climate Dynamics* **34**, 311–472, https://doi.org/10.1007/s00382-008-0507-2.

[16] Brander, L., K. Rehdanz, R. Tol, P. Beukering, and J. van Pieter. 2009. The economic impact of ocean acidification on coral reefs, ESRI Working Paper No. 282, The Economic and Social Research Institute (ERSI), Dublin, http://hdl.handle.net/10419/28758, accessed May 20, 2019.

[17] International Standards Organization. 2019. Country Codes Collection. https://www.iso.org/publication/PUB500001.html, accessed December 15, 2019.

[18] Ding, C., and C. Singer. 2022. Global heat balance model parameter calibration. University of Illinois Program in Arms Control and International Security report ACDIS//ACDIS DIN:4.2022, https://acdis.illinois.edu/system/files/2022-08/CAGE22R4Fronted24Jul.pdf, accessed December 1, 2023.

[19] Food and Agricultural Organization of the United Nations, Statistical Division. 2023. Food and agricultural data, production, value of agricultural production, gross production value (constant 2014–2016 thousand I$, FAOSTAT_data_en_2-18-2023.csv, accessed February 19, 2023.

[20] Intergovernmental Panel on Climate Change Working Group 1. 2013. *Climate Change 2013: The Physical Science Basis*, Section 12.4.5, Changes in the water cycle.

[21] Satish, U., M. Mendell, K. Shekar, T. Hotchi, D. Sullivan, S. Streufert, and W. Fisk. 2015. Is CO_2 an indoor pollutant: Direct effects of low-to-moderate CO_2 concentrations on human decision-making performance. *Environmental Health Perspectives* **120**, 1671–1677.

[22] Snow, S., A. Boyeon, K. Pass, H. Gough, M. King, J. Barlow, C. Noakes, and M. Schraefel. 2019. Exploring the physiological, neurophysiological and cognitive performance effects of elevated carbon dioxide concentrations indoors. *Building and Environment*, **156**, 243–252, https://doi.org/10.1016/j.buildenv.2019.04.010.

[23] American Physical Society Panel on Public Affairs, 2011, Direct air capture of CO2 with chemicals, June 1, https://www.aps.org/policy/reports/assessments/upload/dac2011.pdf, accessed January 15, 2023.
[24] ANSI/ASHRAE. 2019. Ventilation for acceptable indoor air quality, ANSI/ASHRAE Addendum p to ANSI/ASHRAE Standard 62.1-2013, https://www.ashrae.org/File%20Library/Technical%20Resources /Standards%20and%20Guidelines/ Standards%20Addenda/62_1_2013_p_20150707.pdf, accessed May 20, 2019.
[25] O'Keefe, L. 2017. The top 10 most expensive office markets in the world, https://www.bisnow.com/ national/news/office/the-top-10-most-expensive-office-markets-in-the-world-82366, accessed May 20, 2017.
[26] GBD 2017. Troeger, C., M. Forouzanfar, P. Rao, I. Khalil, A. Brown, R. Reiner Jr, N. Fullman, R. Thompson, A. Abajobir, M. Ahmed, M. Alemayohu, N. Alvis-Guzman, A. Amare, C. Antonio, H. Asayesh, E. Avokpaho, A. Awasthi, U. Bacha, A. Barac, B. Betsue, A. Beyene, D. Boneya, D. Malta, L. Dandona, R. Dandona, M. Dubey, B. Eshrati, J. Fitchett, T. Gebrehiwot, G. Hailu, M. Horino, P. Hotez, T. Jibat, J. Jonas, A. Kasaeian, N. Kissoon, K. Kotloff, A. Koyanagi, G. Kumar, R. Rai, A. Lal, H. Razek, M. Mengistie, C. Moe, G. Patton, J. Platts-Mills, M. Qorbani, U. Ram, H. Roba, J. Sanabria, B. Sartorius, M. Sawhney, M. Shigematsu, C. Sreeramareddy, S. Swaminathan, B. Tedla, R. Jagiellonian, K. Ukwaja, A. Werdecker, M. Widdowson, N. Yonemoto, M. Zaki, S. Lim, M. Naghavi, T. Vos, S. Hay, C. Murray, and A. Mokdad. Estimates of global, regional, and national morbidity, mortality, and aetiologies of diarrhoeal diseases: a systematic analysis for the Global Burden of Disease Study 2015, *The Lancet* **17**, 909–948, https://doi.org/10.1016/j.buildenv.2019.04.010.
[27] Roser, M., and H. Ritchie. 2017. Malaria. Our World in Data, https://ourworldindata.org/malaria, accessed August 4, 2019.
[28] Heutel, G., and N. Miller, 2018. Adaptation and the mortality effects of temperature across U.S. climate regions, https://static1.squarespace.com/static/55f6c418e4b03625624b6e69/t/ 5b44b15c88251bce12980304/1531228512816/adaptation.pdf, accessed August 4, 2019; c.f. Heutel, G., N. Miller, and D. Molitor. 2017, NBER Working Paper No. 23271 abstract, https://www.nber.org/papers/w23271, accessed January 23, 2023.
[29] Congressional Budget Office. 2009. The costs of reducing greenhouse-gas emissions, Economic and Budget Issue Brief, https://www.cbo.gov/sites/default/files/111th-congress-2009-2010/reports/11-23-greenhousegasemissions_brief.pd, accessed July 18, 2019.
[30] World Resources Institute. 2009. Emissions reductions under H.R. 2454, the American Clean Energy and Security Act, 2005–2050. http://www.wri.org/usclimatetargets, https://www.wri.org/resources/charts-graphs/emission-reductions-under-hr-2454-american-clean-energy-and-security-act, accessed July 18, 2019.
[31] Ding, C., and C. Singer. 2022. Climate Action Game Experiment motivation and role of radiative forcing, University of Illinois at Urbana-Champaign Program in Arms Control and Domestic and International Security Research Reports ACDIS//ACDIS DIN:1, https://acdis.illinois.edu/systemfiles/2022-08/CAFE22R1Fronted24Jul.pdf, accessed December 1, 2023.
[32] Chen, N., 2021. Conformity and confirmation: Group decision-making in foreign policy, University of Illinois Ph.D. thesis, http:hdl.handle.net/2142/110701.
[33] Laasko, A., U. Neimeier, D. Visioni, S. Tilmes, and H. Kokkola. 2022. Dependency of the impacts of geoengineering on the stratospheric sulfur injection strategy–Part 1: Intercomparison of modal and sectional aerosol modules, *Atmospheric Chemistry and Physics* **22**, 93–118, https://doi.org/10.5194/acp-22-93-2022.
[34] Federal Reserve Bank of Minneapolis. 2023. Consumer Price Index, 1913-, https://www.minneapolisfed.org/about-us/monetary-policy/inflation-calculator/consumer-price-index-1913-accessed January 3, 2023.
[35] Atalla, T., S. Gualki, and A. Lanzo. 2017. A global degree days database for energy-related applications. *Energy* **143**, 1048–1055, https://doi.org/10.1016/j.energy.2017.10.134.
[36] United Nations Statistical Division. 2019. Surface areas, in km^2 from https://unstats.un.org/unsd/databases.htm, accessed March 24, 2019; as of January 23, 2023 available in 1000s of km^2 in Table T02 of Population, density and surface area at https://data.un.org.
[37] American Institute of Physics. 2022. The discovery of global warming, https://history.aip.org/climate/timeline.htm, accessed January 21, 2023.
[38] United Nations, Department of Economic and Social Affairs, Population Division. 2019. World Population Prospects 2019, custom data acquired via website https://population.un.org/wpp/, accessed August 24, 2019.
[39] Singer, C., T. Rethinaraj, S. Addy, D. Durham, M. Isik, M., M.Khanna, B. Keuhl, J. Luo, W. Quimio, R. Kothavari, D. Ramirez, J. Qiang, J. Sheffran, T. Tiouririne, and J. Zhang. 2008. Probability distributions for carbon emissions and atmospheric response, *Climatic Change* **88**, 309–342, https://doi.org/10.1007/s10584-008-9410-4.
[40] Maddison, A. 2010. Historical Statistics of the World Economy: 1-2008 AD, http://www.ggdc.net/maddison/oriindex.htm, accessed August 22, 2019.
[41] Maddison, A. 2003. *The World Economy: Historical Statistics*, Paris: Organisation for Economic Cooperation and Development, https://doi.org/10.1787/9789264104143-en.

[42] International Monetary Fund. 2022. World Economic Outlook Database, October, https://www.imf.org/en/Publications/WEO/weo-database/2022/October, accessed January 6, 2023.
[43] International Monetary Fund. 2019. World Economic Outlook Database, October, https://www.imf.org/en/Publications/SPROLLs/world-economic-outlook-databases#sort=%40imfdate%20descending accessed February 15, 2020.
[44] Singer, C. 2017. Is a naval nuclear arms race with China inevitable? University of Illinois Program in Arms Control & Domestic and International Security Report ACDIS//ACDIS SING:1.2017, https://acdis.illinois.edu/system/files/2020-10/Naval-Nuclear-Arms-China.pdf, accessed December 1, 2023.